Water Resources Research

RESEARCH ARTICLE
10.1029/2018WR023265

Special Section:
Advancing process representation in hydrologic models: Integrating new concepts, knowledge, and data

# Characterizing the Fluxes and Age Distribution of Soil Water, Plant Water, and Deep Percolation in a Model Tropical Ecosystem

**Jaivime Evaristo[1,2], Minseok Kim[3,4], Joost van Haren[4], Luke A. Pangle[5], Ciaran J. Harman[3], Peter A. Troch[4,6], and Jeffrey J. McDonnell[7,8]**

[1]Copernicus Institute of Sustainable Development, Utrecht University, Utrecht, Netherlands, [2]College of Natural Resources and Environment, Northwest A&F University, Yangling, China, [3]Department of Environmental Health and Engineering, The Johns Hopkins University, Baltimore, MD, USA, [4]Biosphere 2, University of Arizona, Tucson, AZ, USA, [5]Department of Geosciences, Georgia State University, Atlanta, GA, USA, [6]Department of Hydrology and Atmospheric Sciences, University of Arizona, Tucson, AZ, USA, [7]Global Institute for Water Security, School of Environment and Sustainability, University of Saskatchewan, Saskatoon, Saskatchewan, Canada, [8]School of Geography, Earth, and Environmental Sciences, University of Birmingham, Birmingham, UK

**Abstract** Recent field observations indicate that in many forest ecosystems, plants use water that may be isotopically distinct from soil water that ultimately contributes to streamflow. Such an assertion has been met with varied reactions. Of the outstanding questions, we examine whether ecohydrological separation of water between trees and streams results from a separation in time, or in space. Here we present results from a 9-month drought and rewetting experiment at the 26,700-$m^3$ mesocosm, Biosphere 2-Tropical Rainforest biome. We test the null hypothesis that transpiration and groundwater recharge water are sampled from the same soil volume without preference for old nor young water. After a 10-week drought, we added 66 mm of labeled rainfall with 152‰ $\delta^2H$ distributed over four events, followed by background rainfall (−60‰ $\delta^2H$) distributed over 13 events. Our results show that mean transit times through groundwater recharge and plant transpiration were markedly different: groundwater recharge was 2–7 times faster (~9 days) than transpired water (range 17–62 days). The "age" of transpired water showed strong dependence on species and was linked to the difference between midday leaf water potential and soil matric potential. Moreover, our results show that trees used soil water (89% ±6) and not the "more mobile" (represented by "zero tension" seepage) water (11% ±6). The finding, which rejects our null hypothesis, is novel in that this partitioning is established based on soil water residence times. Our study quantifies mean transit times for transpiration and seepage flows under dynamic conditions.

**Plain Language Summary** Recent studies suggest that plants use a type of water that is different to the water that recharges the ground, a phenomenon described as the two water worlds. It is unclear, however, whether these waters are segregated in space or in time. That is, do plants draw water from parts of the soil different to groundwater recharge, or do plant water withdrawals happen at a different time from groundwater recharge? Evidence from well-controlled experiments is badly needed because the two water worlds, if true, means that our understanding of the water cycle is incomplete. Here we perform a 9-month drought and rainfall experiment, taking fingerprints of the water molecule, to follow a raindrop from the moment it enters the ground through to its exit via plants or groundwater recharge. Results point to two main discoveries: (1) the travel time of water via root water uptake is much longer than the travel time of water leading to groundwater recharge and (2) the water taken by tree roots comes from parts of the soil that are different to the water leading to groundwater recharge. These discoveries show the segregation of these two components of the water cycle in space and in time.

**Key Points:**
- Root water uptake is derived from the less mobile water in the soil matrix, different to the more mobile water component in soils. The transit times ("ages") of water taken by roots are older than seepage ("groundwater recharge") water by a factor of 2 to 7
- Ecohydrological separation suggests that time-sensitive sampling and modeling techniques are critical for understanding the water cycle
- Species-specific differences in root water uptake transit times suggest that trees should not be treated as simple transport vessels (or "straws") in land surface models

**Supporting Information:**
- Supporting Information S1

**Correspondence to:**
J. Evaristo,
j.evaristo@uu.nl

**Citation:**
Evaristo, J., Kim, M., van Haren, J., Pangle, L. A., Harman, C. J., Troch, P. A., & McDonnell, J. J. (2019). Characterizing the fluxes and age distribution of soil water, plant water, and deep percolation in a model tropical ecosystem. *Water Resources Research*, *55*, 3307–3327. https://doi.org/10.1029/2018WR023265

Received 7 MAY 2018
Accepted 26 MAR 2019
Accepted article online 1 APR 2019
Published online 25 APR 2019

This article was corrected on 17 MAY 2019.



## 1. Introduction

Approximately half of all precipitation that reaches the Earth's critical zone is returned to the atmosphere through plant transpiration (Schlesinger & Jasechko, 2014). However, where plants source this water and how long it remains in the critical zone remains poorly understood. Determining the ages and sources of transpiration water, and stream water, is important to evaluate predictions of mechanistic models of water cycling (Maxwell & Condon, 2016). Recent global-in-scale evidence of ecohydrological

separation (Evaristo et al., 2015; Good et al., 2015), also known colloquially as the *two water worlds* hypothesis (McDonnell, 2014), posits that the water used by vegetation is different to the "more mobile" water in soil, groundwater, and streams. A similar phenomenon was also recently reported using nitrate isotopes (*two nitrate worlds hypothesis*; Hall et al., 2016), supporting the idea that water/nutrient uptake by vegetation and groundwater recharge/nutrient export to streams are separated. Indeed, if ecohydrological separation is real, then the implications for quantifying transit times in streams using current approaches that assume a well-mixed critical zone are profound, because ecohydrological separation is synonymous with an acutely nonwell-mixed critical zone (Brantley et al., 2017; McDonnell et al., 2018).

Originally reported in the Pacific Northwest, USA (Brooks et al., 2010), and later in various sites in the tropics and elsewhere (Evaristo et al., 2016; Goldsmith et al., 2012; Hervé-Fernández et al., 2016), the two water worlds hypothesis has been challenged in certain environments (e.g., Geris et al., 2015; Tetzlaff et al., 2015) and criticized constructively (e.g., Sprenger et al., 2016). Recent commentary supporting the hypothesis (Bowen, 2015; Bowling et al., 2016; Brooks, 2015; McCutcheon et al., 2017) have raised questions related to the purported mechanisms proposed by the original and later authors. Of the many outstanding questions surrounding ecohydrological separation (Berry et al., 2018), one overarching question is explored in this paper: *is ecohydrological separation a separation in time or in space?*

### 1.1. Ecohydrological Separation in Space

The space aspect of ecohydrological separation entails quantifying the source proportions of the isotopic signal that is integrated in the xylem (i.e., plant stem) water. Specifically, this aspect seeks to answer the question, *do trees preferentially draw water from soil micropores over the freely draining water that contributes to groundwater recharge?* Approaches in plant source water quantification using the stable isotopes of water generally fall under two main categories: process-based mixing models and simple linear mixing models (Ogle et al., 2014). Process-based mixing models (e.g., RAPID by Ogle et al., 2004, 2014) integrate stable isotope data and a biophysical model into a Bayesian framework. Where two or three water sources are identified, traditional simple linear mixing models may prove sufficient for explicit representation of sources via simple mass balance (e.g., Brunel et al., 1995; Thorburn & Walker, 1994).

In the simplest case where xylem water may represent an integrated signal of two sources, the proportional contribution of each source may be resolved using a single isotope in a two-source system, mass balance equation (Dawson, 1993; Phillips & Ehleringer, 1995):

$$\delta_{xyl} = f_A\delta_A + f_B\delta_B \tag{1}$$

where $\delta_{xyl}$ is the plant xylem water (either $\delta^2$H or $\delta^{18}$O) and the proportions ($f_A$,$f_B$) of sources (summing to 1) with isotopic signatures ($\delta_A$,$\delta_B$), respectively.

In many if not most cases, however, the number of possible sources—vadose versus saturated zone, different depths in the soil profile, more mobile versus less mobile—far exceeds the number of isotopes in the system, that is:

$$\delta_{xyl} = f_A\delta_A + f_B\delta_B + f_C\delta_C + \cdots f_n\delta_n \tag{2}$$

In such an underdetermined system, where the number of sources is greater than the number of isotopes plus one, the most widely used approach to date is an algorithm called IsoSource (Evaristo & McDonnell, 2017; Phillips & Gregg, 2003). Notwithstanding the widespread use of IsoSource in systems with multiple sources, the method can only provide a range of feasible (not likely) solutions (Parnell et al., 2010). The lack of a robust statistical foundation of an iterative approach, therefore, boosts the case for an alternative method that frames the mixing model atop a solid statistical (i.e., Bayesian) formulation. Quantifying plant water sources is key not only for understanding source apportionment in the critical zone but also for testing the space-based (if any) aspects of *ecohydrological separation*.

### 1.2. Ecohydrological Separation in Time

Earlier research on the two water worlds hypothesis assumed implicitly that transpiration flux is older than the more mobile water pool. For example, Brooks et al. (2010) suggest a serial process whereby

plants use "tightly bound" water after mobile water from large pores and preferential flow paths has drained. Such a conceptual model suggests that transpiration water may be drawn from small pores with water that has been in storage for some time (Soulsby et al., 2016). This runs counter to most catchment modeling studies suggesting that evapotranspiration fluxes are younger (Hrachowitz et al., 2013, 2015; Harman, 2015). The time aspect of ecohydrological separation entails estimating the mean transit time (MTT) from corresponding transit time distribution (TTD) of subsurface water and transpiration. However, no study has yet quantified the transit time of transpired water (except for residence time studies that used $D_2O$ label injection into trees; see later texts) or the transit time of the low-mobility water, barring a recent study that used postbomb tritium as a tracer (Zhang et al., 2017).

The main challenge in estimating MTT with respect to testing ecohydrological separation in time is the lack of direct measurements of water flows into different compartments. In steady state and well-mixed conditions, MTT is the ratio between storage volume ($L^3$) and average water flow ($L^3/T$). Catchment *transit time* is thus the time that a water parcel spends from input as rainfall to output as streamflow or transpiration water (also known as "exit age"). In rainfall-runoff literature, the shape of stream water TTDs and associated MTT provide insight into catchment behavior with implications for runoff generation, nutrient export, and contaminant fate and transport (Hrachowitz et al., 2016; Kirchner et al., 2000; McDonnell et al., 2010). While stream water MTT and TTD have been, and continue to be, a staple of much active research (McGuire & McDonnell, 2015), the other piece of the exit age distribution—namely, plant transpiration—has until now been neglected. Indeed, Soulsby et al. (2016) note that "estimating the age distribution of evaporated waters remains a fundamental research need in order to quantify the total exit age of waters leaving a catchment."

Recently, Harman (2015) and Wilusz et al. (2017) have demonstrated that stream water isotope variability can provide some constraints on the age distribution of transpiration water. These authors proposed that TTDs, based on storage selection functions, provide a framework for capturing tracer transport through evapotranspiration. Nonetheless, sensible parameterizations of these functions could not be validated by direct observation. The only direct observations come from a few studies in the plant ecophysiology literature (e.g., James et al., 2003) where within-tree $D_2O$ labeling has been performed to estimate tracer velocity and ages. James et al. (2003) reported tree water ages for two tropical species in Panama that ranged between 2 (*Cordia alliodora*) and 22 days (*Anacardium excelsum*). A similar range was reported by Meinzer et al. (2006) for two coniferous (Douglas fir and western hemlock) species in southwestern WA, USA, while Gaines et al. (2016) reported a range between 5 and 22 days for four tree species in PA, USA. Together, state-of-knowledge suggests marked variability, amplifying the need for studies that explore plant water age, soil water age, and stream water age altogether, that is, experimentally.

And while TTDs and MTTs are informative, it is important to note that these are not measured per se but rather inferred from conservative geochemical tracers (e.g., $Cl^-$, $^{18}O$, $^{2}H$). The inferential nature of TTD modeling implies, with all its simplifying assumptions (see Kirchner, 2016), that the shape of a TTD can be assumed. Hence, recent work has called for catchment-scale labeling studies to experimentally define the TTD (Harman & Kim, 2014; Klaus et al., 2015; McDonnell & Beven, 2014). Moreover, while experimental and modeling work in rainfall-runoff transit times are now common practice (for review, see McGuire & McDonnell, 2006), rarely, if ever, has the "transit time modeling enterprise" contained rainfall-transpiration tracer parameterization. Similarly, when water transport studies have included isotope labeling in vegetation (e.g., Gaines et al., 2016; James et al., 2003; Meinzer et al., 2006), they have lacked the typically high-resolution sampling in rainfall-runoff experiments (McGuire & McDonnell, 2006), let alone comparison to whole-catchment transit times with explicit labeling and tracking of root water uptake sources (Soulsby et al., 2016). Advances in understanding of whole-catchment transit times, based on controlled experiments, is key not only for understanding mixing and source apportionment in the critical zone but also for testing the time-based (if any) aspects of *ecohydrological separation*. Specifically, this aspect seeks to answer the question, *how do transit times ("ages") of water via root water uptake contrast with water that contributes to groundwater recharge?*

### 1.3. Drivers of Separation and the Need for Controlled Experiments

Furthermore, it is not known how ecohydrological separation in space and time (if any) might change under changing soil moisture conditions. This problem sits at the core of the ecohydrological separation

hypothesis, as distilled in a conceptual model proposed by Brooks et al. (2010). An advance in our understanding of this problem is important because the apparent preference of vegetation for less mobile (soil matrix) over more mobile (e.g., suction lysimetry) water has been explored hitherto in field settings where control for soil moisture states was impossible. For example, Berry et al. (2018) postulated that if the volume of water taken by plant roots is greater than the volume of water sampled via suction lysimetry—as the case might be in a water-limited regime (e.g., drought)—then a mixture of more mobile and less mobile water in the xylem must be likely.

So how can we evaluate and quantify these space- and time-based aspects of ecohydrological separation when boundary conditions in natural catchments are unknown and largely unknowable? In general, experiments that allow for high degree of control over environmental variables at useful space and time scales are needed. What is needed going forward to characterize sources, flow paths and exit time distributions is a practicable combination of control at the growth chamber scale and field-based experiments at the representative elementary volume of the critical zone domain. Such setting is large enough to contain a sufficient range of heterogeneity and thereby satisfy scale requirements. But these experimental scale requirements then come at a cost of not being able to control experimental variables.

Here we take advantage of the 27-m-tall, 1,936-$m^2$ mesocosm Biosphere 2-Tropical Rainforest (B2-TRF) biome that represents a total volume of 26,700 $m^3$. The B2-TRF has soils ranging from 1 to 4 m deep with 23 tree species where much basic ecosystem work has already been completed (Leigh et al., 1999; Rascher et al., 2004; Rosolem et al., 2010; Scott, 1999). As such, the B2-TRF biome represents the ideal scale at which to address fundamental aspects of water sources, flow paths, and transit times through the critical zone, enabling controlled experiments to be designed and implemented in a model biome, but with complete boundary control.

We present results from a 9-month drought and rewetting experiment where we induce water stress on the ecosystem and follow the water uptake patterns of five dominant tree species ($n = 8$). We added 66 mm of labeled rainfall with 152‰ deuterated water distributed over four rainfall events in one week. We then followed the rainfall labeling regime with a total of 87 mm of rainfall (−60‰) distributed over 13 successive events, spaced every 2–3 days. Over the course of this 9-month experiment we tested the null hypothesis that water volumes contributing to groundwater recharge and transpiration are sourced from a single, well-mixed reservoir that occupies pore space from the soil surface to the vertical extent of plant roots. We explored ecohydrological separation in *space* by quantifying the source water proportions in xylem ("mixture") water, using a linear mixing model implemented in a Bayesian framework. We explored ecohydrological separation in *time* by examining TTDs, using the observed breakthrough curves (BTCs) associated with the fluxes to estimate the TTDs. Our specific research questions are the following:

1. Do trees preferentially draw water from soil micropores over the freely draining water that contributes to seepage?
2. How do transit times (ages) of water via root water uptake contrast with deep percolation or seepage?

## 2. Materials and Methods

### 2.1. Biosphere 2 Tropical Rainforest

Biosphere 2 (B2) is a large-scale Earth science research facility operated and owned by the University of Arizona, Tucson (Arizona, USA). It consists of five biomes, including the tropical rainforest (B2-TRF) biome where we conducted this study (Figure 1). Constructed between 1990 and 1991, the B2-TRF is a 1,936-$m^2$ mesocosm with a total air volume of 26,700 $m^3$ (Rascher et al., 2004) and total soil volume of ~3,000 $m^3$, all enclosed in a glass and steel framework above ground and a concrete basin lined with stainless steel below ground. The distance between the lowest soil level and the highest point in the enclosed, pyramidal glass structure is ~27 m. Rainfall, humidity, and temperature inside the B2-TRF are controlled to reflect climatic conditions that are comparable to natural rainforests (Arain et al., 2000; Leigh et al., 1999).

The soil inside the Biosphere 2 rainforest was constructed from local sources with 1,995 $m^3$ of topsoil (Scott, 1999) overlaying ~1,000-$m^3$ granite gravel. Soil depth ranges from ~1 to 3.5 m, with most trees sampled for this study growing in soils between 2.4- and 3-m depth. *Pterocarpus indicus* was in an area with only ~1-m soil depth and a small stream, which the tree had access to, running through the area. About 0.9 m of topsoil


**Figure 1.** Study site. (a) Aerial photo of the Biosphere 2 facility, Oracle, AZ, USA; the Tropical Rainforest (B2-TRF) biome is indicated by the white arrow. (b) Photo taken inside B2-TRF showing understory species and woody vines typical of wet tropical rainforests. (c) One of three soil pits where soil measurements (soil moisture and soil water potential) and soil isotope sampling were made; in the photo are three undergraduate research assistants (clockwise: Fatima Olmos-Flores and Ietza Gonzalez-Silva from Mexico, Meghan McDonnell from OR, USA) who helped in the experiment. (d) Photo taken inside one of the three soil pits, showing the acrylic glass (Plexiglas) walls and holes to accommodate instrumentation and sampling; also shown are the instrumentation for volumetric water content measurement (5TM Decagon Devices WA, USA), and soil water potential (T4e UMS GmbH Germany).

was created from a mix of 50% silt loam, 25% gravely sand, and 25% coarse organic material (Scott, 1999). Below that the soil consisted of granite gravel, with many pieces greater than 10 $cm^3$. The soil texture and course soil particles increased strongly (from ~20 to 50%), which suggests that the water holding capacity greatly decreased, thus reducing the water available for plant uptake below 65 cm. Tree roots were found predominantly in the topsoil (now 65 cm on average) when we dug the 1- by 1.5-m soil pits in 2009 and 2010) with the highest fraction (~60%) found at the top 15–20 cm of the soil profile.

The plant community consists of a mix of trees, vines, and herbs designed to mimic a tropical rainforest (Leigh et al., 1999). The plants were derived from multiple locations closely representing a pan-tropical distribution. The largest trees currently reach to ~25 m in height and ~50 cm in diameter. This study focuses on soil water, deep percolation, and five tree species (described in detail below), and their partitioning of water sources and its drivers during and after a controlled drought. This study places emphasis on the use of water stable isotopes as well as soil moisture and water potential measurements. For a detailed study with emphasis on atmospheric forcing and vegetation response at the B2-TRF, the interested reader is directed to Rosolem et al. (2010).

Artificial rainfall, applied every 3–4 days, is delivered using overhead sprinklers that are equally distributed in four quadrants. During normal conditions (i.e., without an ongoing experiment), the B2-TRF receives an annual rainfall of ~1,300 mm (3.6 mm/day) with relatively constant $\delta^2H$ and $\delta^{18}O$ values (mean ± 1 SD) of −60.2 ± 4.2‰ and −8.3 ± 0.75‰, respectively. Rainfall amounts are monitored through in line flowmeters before the water enters the rainforest. Operating in "flow through mode" where outside drier air is vented through the system and humidity fixed between 70% and 85%, an inversion layer exists above the mean canopy level resulting in two distinct daytime humidity regimes. Turbulence is negligible suggesting that the primary atmospheric transport process is a combination of mass flow and molecular diffusion (Arain et al., 2000). Rainfall events take place usually during nighttime so that isotopic enrichment of throughfall and interception via evaporation water are minimal.

### 2.2. Drought and Rewetting Experiment

To be able to assess the possible changes in source water apportionment in the dominant canopy species, we performed a drought experiment by eliminating precipitation. This was achieved by closing all valves on the water pipe going into the rainforest. The drought lasted for 68 days between 23 July and 29 September 2014. During rewetting that began 30 September 2014, we introduced a 99.5% deuterium oxide ($D_2O$) label (Cambridge Isotopes, Cambridge, MA, USA) into the sprinkler ("rainfall") system. Using the information from a 2002 drought-rewetting exercise at B2-TRF, we calculated that ~130,000 L of rainfall was necessary to generate subsoil drainage ("seepage") and allow the soil moisture down to 60 cm to recover. This translated to a total of 66 mm of labeled rainfall with 152‰ $\delta^2H$, distributed over four events (mean 16.5 mm per event) including the 30 September rain: 1, 5, and 7 October. This was followed by a total of 87 mm of rainfall (−60‰ $\delta^2H$) distributed over 13 events that were spaced every 2–3 days. The amount and intensity of the latter rainfall events were calculated to revert the B2-TRF system back to its normal rainfall regime.

### 2.3. Environmental Monitoring and Sampling

The environmental conditions within the B2-TRF are monitored along a vertical profile with measuring heights of 1, 3, 7, 13, and 20 m above the soil surface. The current locations are based on the locations used between 1998 and 2003 (Rascher et al., 2004). At each height we measured light (PAR sensor and Pyranometer, SQ-110 and SP-110, Apogee, Logan, UT, USA), relative humidity and temperature (Vaisala HMP 45c sensor, Vaisala, Vantaa, Finland, covered by a 10-plate gill solar radiation shield), and wind speed (anemometer, Met One Instruments, Grants Pass, OR, USA). All data was collected at 15-min intervals with a datalogger and multiplexers (Campbell Scientific Instruments, Logan, UT, USA) and automatically downloaded to a server at Biosphere 2.

From the temperature and relative humidity measurements along the tower profiles we derived the vapor density (VD, $g/m^3$) at each time step for four different height zones within the rainforest, which was then used to calculate the evapotranspiration (ET). ET inside the B2-TRF not only represents soil evaporation and plant transpiration but also includes the condensation and evaporation of water on the glass and the frames supporting it. Changes in ET within the rainforest can be calculated from

$$ET = \Delta VD + (VD_{out} - VD_{in})V_{flow} + Cond_{AHU} \quad (3)$$

where ΔVD represents the change in vapor pressure within the B2-TRF with each time step; $VD_{in}$ and $VD_{out}$ represent the vapor pressure of the air flowing in (based on Vaisala HMP 45c measurements of the intake air) and out (based on the top tower Vaisala HMP 45c measurements, since the air was vented out of the top of the rainforest), respectively; $V_{flow}$ represents the air flow into the rainforest (monitored with sonic anemometers); and $Cond_{AHU}$ represents the condensation in the air handler units (AHU; large air conditioners; Figure 2) measured by the difference in VD of the air flowing in and out and the total volume of air flow.

There are three 1 × 1.5-m soil pits, with depths varying between 1 and 3 m (Figure 2). The four walls consist of acrylic glass (Plexiglas) in an aluminum frame. Holes were made into the Plexiglas walls to accommodate instrumentation and sampling. Volumetric water content (VWC) was determined by measuring the dielectric constant of the soil using capacitance/frequency domain technology (5TM Decagon Devices WA, USA), and was calibrated with the gravimetric method. Soil water potential (SWP) was measured at the same

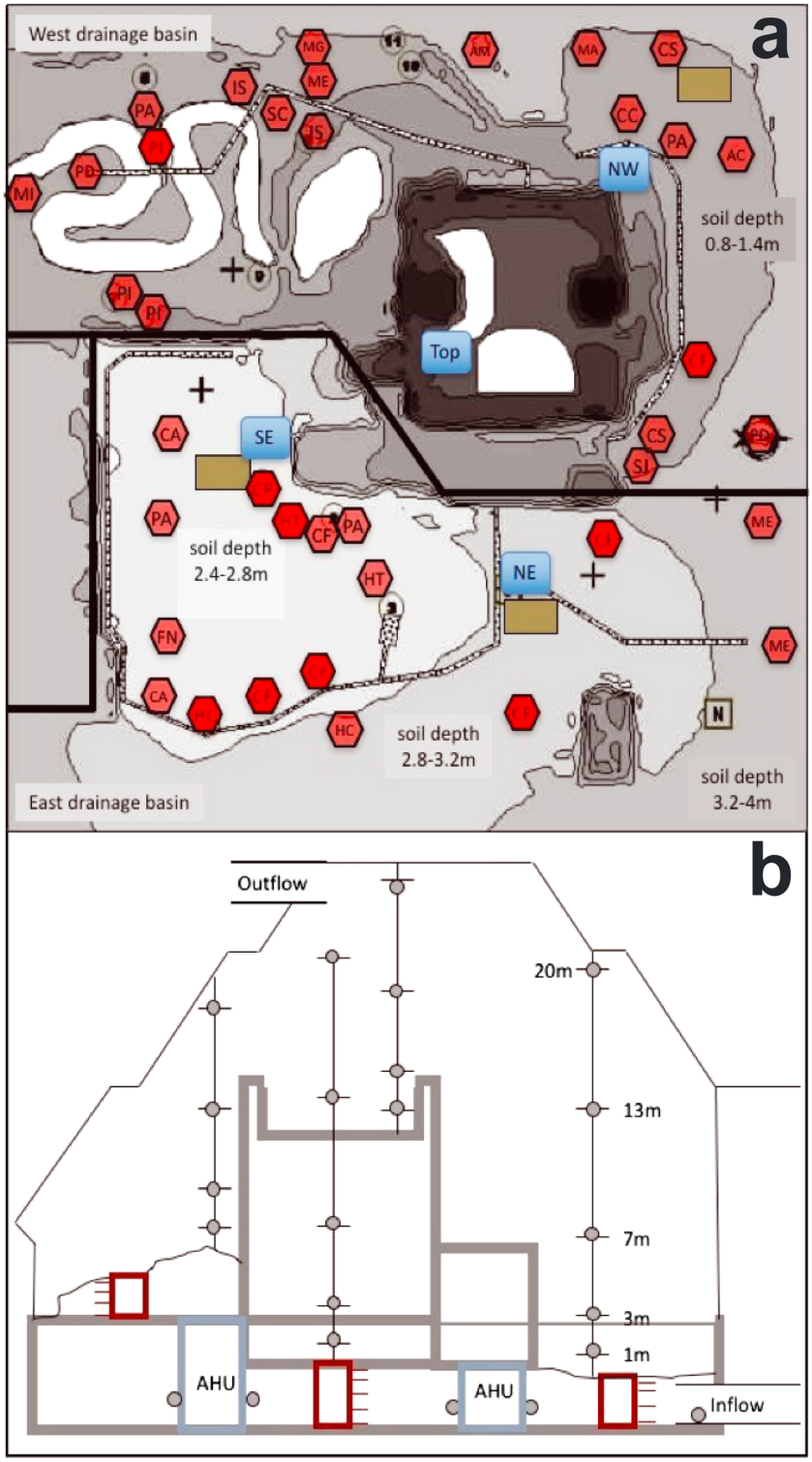


**Figure 2.** Map (a) and cross section (b) of the Biosphere 2 rainforest. The map shows the locations of the main trees (hexagons) and focal trees for this study (bright red fill), towers (blue squares), soil pits (tan rectangles), delineation of the east and west drainage basins, and approximate soil depths. The shading in the maps indicates rough surface heights. The cross section shows the towers with temperature and humidity sensors (gray circles), soil pits (red squares with dashes which denote the sensor heights), inflow-outflow system, and air handler units (AHU; blue squares).

**Table 1**
*Environmental and Isotope Parameters Used in the Craig-Gordon Model (Craig & Gordon, 1965) (Mean, Lower, and Upper 95% Bias-Corrected Bootstrap Percentile Intervals) and Resulting $\delta_E$ Values (See Text S1)*

| Parameter | Mean | Lower 95% | Upper 95% |
|---|---|---|---|
| $\delta_{pan}$ | −5.46 | −5.93 | −4.93 |
| Relative humidity | 0.7702 | 0.7626 | 0.7777 |
| Temperature (°C) | 23.20 | 23.12 | 23.27 |
| $\delta_A$ | −8.26 | −8.43 | −7.63 |
| $\delta_E$ | −9.94 | −11.73 | −9.39 |

*Note*. Other model parameters $\varepsilon$ and $\varepsilon_K$ are as stated in the text.

depths (15, 25, 55, 65, 100, 130, and 150 cm) with recording tensiometers (T4e UMS GmbH Germany). T4e measurement range is between +100 and −85 kPa with an accuracy ±0.5 kPa.

To estimate the water balance, storages and flows were sampled for isotopic analysis and subsequent mass budget analysis. We collected throughfall samples during one, seven, and six events in February, June, and July 2014, respectively, before the drought (see section 2.4). Seepage samples (representing "zero tension" groundwater recharge) from collector pipes that drain the overlying mesocosm were also collected manually during and around the same times as for rainfall sampling and at higher frequency during postdrought (rewetting; see frequency of seepage water sampling in Text S1). While it was ideal to collect soil and xylem water samples around the same times as rainfall and seepage sampling, logistical and cost considerations proved to be prohibitive. Nevertheless, we sampled for bulk soil water isotopes weekly by collecting soil samples (three replicates each) at 15, 25, 35, 55, 100, 130, and 250 cm. Although each soil pit was covered by a 1.5-cm-thick metal sheet when no sampling was performed, care was taken during each sampling by scraping ~3 cm of soil off the face of the wall at respective depths. This was done to ensure that we were not sampling for evaporatively enriched soil water at the soil face.

Weekly stem ("xylem") water samples were taken from the part of stems with mature bark closest to the main branch (following Dawson, 1993) to minimize the effect of evaporative enrichment by water loss through unsuberized stems. Stem samples were collected (three replicates each) using clipping just below canopy height (~15 m) via bosun's chair from five canopy species: *Ceiba pentandra* ($N = 2$, DBH = 36, and 53 cm), *Clitoria racemosa* ($N = 4$, DBH = 29 ± 3 cm), *Hura crepitans* ($N = 1$, DBH = 45 cm), *Hibiscus elatus* ($N = 1$, DBH = 28 cm), and *Pterocarpus indicus* ($N = 1$, DBH = 24 cm).

Water from bulk soil and stem samples were extracted using cryogenic vacuum distillation method. Isotope analyses of all stem water samples were performed using isotope ratio mass spectrometry at the University of Victoria (Alberta Innovates-Technology Futures) due to possible spectral contamination of plant water. Isotope analyses of bulk soil, rainfall, and seepage water samples were performed using isotope ratio infrared spectroscopy (LGR OA-ICOS CA, USA) at McDonnell Watershed Hydrology Lab. Laboratory precision at both University of Victoria and McDonnell Lab was ±1‰ and ±0.2‰ $\delta^2H$ and $\delta^{18}O$, respectively.

### 2.4. Plant Source Water

We compared the isotopic composition ($\delta^{18}O$) of bulk soil water at respective sampling depths within each moisture period (drought and postdrought). Finding no statistical difference in $\delta^{18}O$ of bulk soil across depths within a moisture period prior to and during the drought ($P > 0.05$, Tukey's honestly significant difference), we discretized the subsurface into five possible plant water sources—four bulk soil water (10–20, 20–40, and 40–60 cm, prerewetting) and seepage (zero tension, more mobile) water—using only rewetting (postdrought) data when isotopic differences were apparent.

### 2.5. Isotope Mass Balance Calculation

Major components of the water balance at the B2-TRF include rainfall (P), soil water (S), subsoil drainage or seepage (L), interception (I), soil evaporation (ε), and root water uptake (T). We know the mass and isotopic composition associated with each component of the water balance except for I (Table 1, Text S1). The isotope mass balance, calculated as cumulative mass flows over the length of the entire experiment, was formulated as follows:

$$\boldsymbol{m}_P+\boldsymbol{m}_{S,i}=\boldsymbol{m}_L+\boldsymbol{m}_I+\boldsymbol{m}_{S,f}+\boldsymbol{m}_\varepsilon+\boldsymbol{m}_T \tag{4}$$

and

$$\boldsymbol{\delta}_P\boldsymbol{x}_P+\boldsymbol{\delta}_{S,i}\boldsymbol{x}_{S,i}=\boldsymbol{\delta}_L\boldsymbol{x}_L+\boldsymbol{\delta}_I\boldsymbol{x}_I+\boldsymbol{\delta}_{S,f}\boldsymbol{x}_{S,f}+\boldsymbol{\delta}_\varepsilon\boldsymbol{x}_\varepsilon+\boldsymbol{\delta}_T\boldsymbol{x}_T \tag{5}$$

where $\boldsymbol{m}$ is the mass, $\boldsymbol{\delta}$ is the isotopic composition, and $x$ represents the fraction of corresponding component in the water balance. Soil water mass is represented by subscripts *S,i* and *S,f* to indicate the initial soil water

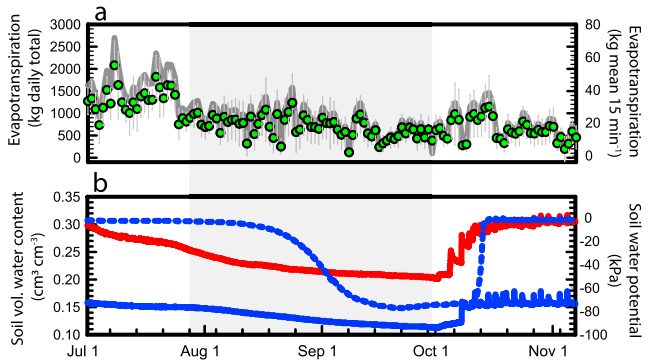


**Figure 3.** Modeled ecosystem-scale evapotranspiration and soil moisture and water potential. Gray shaded area represents drought period (23 July to 29 September 2014). (a) Ecosystem-level evapotranspiration amount. Left axis is daily total in kg (gray curves), and right axis are 15 min totals (filled green circles); error bars represent 1 SD. Note that the evapotranspiration inside the greenhouse also includes the condensation and evaporation of water from the glass and supporting frame. (b) Soil water content (left axis) at 25 (red solid line) and 65 cm (blue solid line) and soil matric potential (right axis, blue dashed line) at 65 cm.

mass *i* prior to rainfall and the final soil water mass *f*. $\delta_{S,i}$ and $\delta_{S,f}$ were calculated using the weighted isotopic composition at each soil layer (following Sutanto et al., 2012):

$$\delta_{S,i} = \delta_{S,f} = \frac{\sum_{j=1}^{n}(\delta_{sj}\cdot z_j\cdot\theta_j)}{\bar{\theta}\cdot Z_{total}} \quad (6)$$

where $n$ is the number of soil layer, $\delta_{sj}$ is the isotopic composition at corresponding layer $j$, $z_j$ is the corresponding soil thickness at layer $j$, $\theta_j$ is the soil water content at layer $j$, $\bar{\theta}$ is the average soil water content, and $z_{total}$ is the total depth. For purposes of closing the water balance, we considered three depths 25, 65, and 150 cm because continuous VWC data from these depths were ascertained as reliable, that is, without instrument reading issues (see water balance details in Text S1).

Water balance terms (in mm per week) are the following: rainfall, 36 mm (12 mm per event times three events per week); seepage, 4.2 mm (0.6 mm per day); soil evaporation, 2.66 mm (0.38 mm per day derived from pan evaporation experiment); transpiration, 7.14 mm (1.02 mm per day derived from ecosystem-level modeled transpiration; Figure 3a); and soil water, 369 mm (integrated at three depths 25, 65, and 150 and derived from respective VWC data). Total mass, in depth terms ($m_{total} = m_P + m_{S,i}$), is 405 mm. Ecosystem-level modeled transpiration (in kg) was converted to depth water (in mm) by assuming that 1 $m^3$ of water is approximately equal to 1,000 kg and then dividing by the surface area of B2-TRF.

### 2.6. Ecohydrological Separation in Space: Bayesian Inference

We determined the source water proportions in xylem (mixture) water by using a linear mixing model implemented in a Bayesian framework. We employed the stable isotope analysis in R Bayesian mixing model statistical package (Parnell et al., 2010) to determine the most likely proportion of xylem water from various depths in the soil profile using Markov chain Monte Carlo methods. We discretized the soil profile into five possible plant water sources: three soil depth intervals (10–20, 20–40, and 40–60 cm), representing respective soil water isotopic composition during rewetting; an integrated depth (10–60 cm), representing soil water isotopic composition prior to rewetting; and seepage (zero tension, "mobile") water during rewetting. Soil and seepage water data were available at eight sampling time points, spanning 70 days (10 weeks): 30 September, 2 October, 7 October, 14 October, 21 October, 28 October, 4 November, and 9 December. Source water isotopic compositions (mean ± 1 SD) are shown in Table 2; xylem water isotopic compositions are shown in Table 3.

The model was run with 500,000 iterations (discarding the first 50,000) and a source water's most likely contribution (i.e., the mean of the posterior distribution of the Markov chain Monte Carlo simulation) to xylem water was obtained. A uniform (i.e., noninformative prior) distribution was used in the model run. The stable isotope analysis in R method was an appropriate treatment of our data because of the number of possible sources considered. Evaristo et al. (2017) showed that a Bayesian approach constrains the uncertainty estimates better than simple mass balance (e.g., Brunel et al., 1995) when maximizing the difference between

**Table 2**
*Source Water $\delta^2H$ Isotopic Compositions (Mean ± 1 SD)*

| Source | 30 September | 2 October | 7 October | 14 October | 21 October | 28 October | 4 November | 9 December |
|---|---|---|---|---|---|---|---|---|
| 10–20 cm | −4.85 ± 27 | 62.8 ± 52 | 53.6 ± 45 | 0.84 ± 38 | −25.6 ± 38 | −40 ± 23 | −55.8 ± 5.7 | −63.8 ± 2.3 |
| 20–40 cm | −32.8 ± 25 | 14.5 ± 60 | 31 ± 48 | −0.89 ± 22 | −27.3 ± 26 | −42.7 ± 12 | −53.6 ± 4.2 | −65.4 ± 12.8 |
| 40–60 cm | 70.3 ± 1 | 8.8 ± 5.1 | 8.4 ± 1.5 | −2.8 ± 2.9 | −8.9 ± 3 | 0.64 ± 3.1 | −21.8 ± 1.1 | −61.6 ± 1.3 |
| Prerewetting | −62.2 ± 2.8 | −62.2 ± 2.8 | −62.2 ± 2.8 | −62.2 ± 2.8 | −62.2 ± 2.8 | −62.2 ± 2.8 | −62.2 ± 2.8 | −62.2 ± 2.8 |
| Seepage | 63.8 ± 38 | 73.5 ± 17 | 63.1 ± 8.6 | −34.8 ± 13 | −42.4 ± 6.5 | −38.1 ± 0.69 | −45.8 ± 4.8 | −45.1 ± 1.1 |

**Table 3**
*Xylem Water $\delta^2H$ Isotopic Compositions (Mean ± 1 SD)*

| Species | 30 September | 2 October | 7 October | 14 October | 21 October | 28 October | 4 November | 9 December |
|---|---|---|---|---|---|---|---|---|
| *C. pentandra* | −56.5 ± 3.9 | −49.0 ± 2.2 | −51.7 ± 1.4 | −57.7 ± 4.8 | −52.7 ± 3.1 | −57.4 ± 3.6 | −61.1 ± 4.4 | −51.1 ± 2.1 |
| *C. racemosa* | −56.9 ± 3.5 | −26.2 ± 10 | −26.7 ± 15 | −6.4 ± 6.2 | −27.1 ± 7.1 | −34.7 ± 4.4 | −47.7 ± 4.4 | −55.1 ± 2.6 |
| *H. crepitans* | −62.9 ± 0.8 | −48.7 ± 0.5 | −57.1 ± 0.2 | −56.4 ± 4.9 | −45.2 ± 3.9 | −39.9 ± 0.7 | −39.0 ± 1.3 | −43.9 ± 0.8 |
| *H. elatus* | −61.6 ± 2.7 | −19.0 ± 4.9 | 14.1 ± 1.0 | −1.1 ± 0.6 | −23.0 ± 0.8 | −35.4 ± 0.8 | −38.9 ± 1.2 | −51.8 ± 0.3 |
| *P. indicus* | −63.8 ± 0.6 | −47.0 ± 3.8 | −27.9 ± 2.3 | −38.2 ± 1.9 | −43.5 ± 1.0 | −44.9 ± 16 | −58.6 ± 2.3 | −61.9 ± 2.2 |

sources is not possible. The use of combined bulk soil water values also leads to more constrained and less diffuse solutions (Phillips et al., 2014) than if we assigned sources with statistically insignificant differences.

While we collected weekly bulk soil and stem water samples for isotope analyses before and during the drought, 2 July to 29 September 2014, spanning 89 days (~13 weeks), root water uptake modeling was performed only on rewetting data because the isotopic differences prior to rewetting (i.e., predrought and drought) were not statistically significant.

### 2.7. Ecohydrological Separation in Time: TTDs

The differences in time scales of transport dynamics toward each outflux could be revealed by examining TTDs. We used the observed BTCs associated with the fluxes to estimate the TTDs. In this study, we estimated the TTDs using the flow-weighted time approach (Ali et al., 2014; Kim et al., 2016). This approach was done to estimate approximate transit times associated with each outflux and their relative differences. A key assumption in this approach is that partitioning between flow pathways—toward seepage or transpiration—is negligible, and therefore, the partitioning of the labeled water particles into each outflux is not a function of time either. This assumption means that the effect of fluctuating storage on the time variability of a TTD must also be assumed to be negligible. While the time variability of TTDs caused by fluctuating in-and-out fluxes can be considered in this approach, detailed information on seepage outflux was not available in this case. An additional assumption was therefore introduced regarding the temporal structure of outflux—the perturbation to the seepage flux caused by a rainfall event is relaxed as an exponential recession with a 0.5-day time scale (which is fitted to occasional seepage flux measurements). Temporal structure of the transpiration fluxes was assumed to be uniform. The periodic rainfall events irrigating the rainforest occurred approximately every 2 or 3 days for over 93% of the whole analysis period, so this assumption alone is unlikely to significantly affect the comparison among the estimated TTDs if the differences are large. The TTDs were estimated by choosing a specific form for the TTDs in the flow-weighted time. The BTC was resimulated by transforming the injection concentration time series into flow-weighted time, convolving the transformed time series with the TTD, then transforming the result back into clock time. Parameters of the TTDs were estimated by comparing the observed and predicted BTC (see Text S1).

## 3. Results

### 3.1. Environmental Conditions

Total ecosystem evapotranspiration (plant transpiration, evaporation, and condensation in the structure) predrought ranged between 900 and ~2,700 kg/day (1,733 ± 389 kg/day). During the drought, ecosystem-level evapotranspiration decreased to between 100 and ~1,500 kg/day (877 ± 319 kg/day). Evapotranspiration amount recovered slightly during the first 2 weeks following rewetting (similar to early and middrought levels) but maintained at subdued levels (635 ± 296 kg/day) over the course of the record (Figure 3a).

Soil volumetric water content (VWC) at 25-cm predrought ranged between 0.26 and 0.31 $cm^3/cm^3$ (0.28 ± 0.01 $cm^3/cm^3$; Figure 3b). During the drought, VWC at 25 cm decreased to between 0.20 and 0.26 $cm^3/cm^3$ (0.22 ± 0.02 $cm^3/cm^3$). VWC at 25 cm began to recover to predrought levels ~8 days following rewetting. It fully recovered (i.e., stabilized) to predrought levels at ~14 days. Water content at 65-cm predrought ranged between 0.15 and 0.16 $cm^3/cm^3$. During the drought, this decreased to between 0.11 and 0.15 $cm^3/cm^3$ (0.13 ± 0.01 $cm^3/cm^3$). Like water content at 25 cm, VWC at 65 cm began to recover to predrought levels ~8 days following rewetting and stabilized at ~14 days. SWP predrought

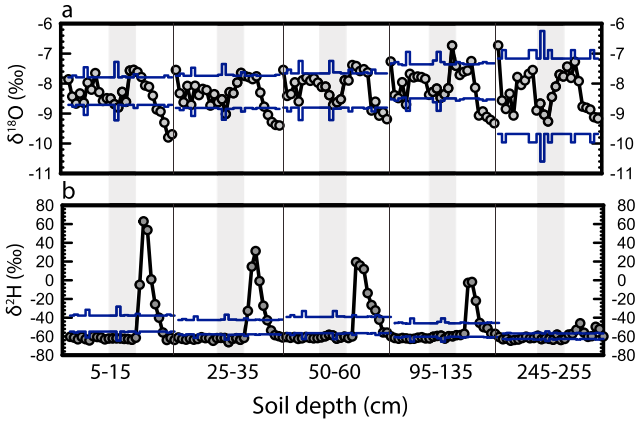


**Figure 4.** Control chart of soil water isotopic composition for the entire study period. (a) $\delta^{18}O$ and (b) $\delta^{2}H$. A control chart indicates whether or not a soil water isotopic composition value is within a range of statistical variation. The range is defined by the upper and lower control limits (bold dark blue lines), which set the range of variation that is to be expected in the summary statistic when the measurement is in statistical control. The horizontal axis represents the depth within the soil profile, grouped according to the range of sampling interval and arranged in time series (2–28 July predrought, 29 July to 29 September drought, 30 September to 1 December rewetting). Shaded gray region represents the extent of drought. Each point represents a summary statistic, that is, average of all measurements from a corresponding soil depth. A point outside the upper or lower control limits indicates a measurement that may be caused by factors that did not have an apparent influence over the points within the range, and therefore a useful indicator of anomaly in the data series.

ranged between −3 and −2 kPa (20- to 30-cm $H_2O$). During the drought, this decreased to between −77 and −3 kPa (30- to 785-cm $H_2O$). SWP recovered to predrought levels ~14 days following rewetting. We note that of the seven SWP recording tensiometers, only one (65 cm; Figure 3b) generated data that were deemed reliable. The rest encountered cavitation issues, with sensor readings gradually dropping until the air entry of the ceramic was reached, after which the values dropped wildly to zero.

Soil water $\delta^{18}O$ for the period illustrated ranged between −9.8‰ and −6.7‰ (Figure 4a). The predicted range (i.e., upper and lower control limits) for the first four depth groups ≤135 cm were comparable, ranging between −9.2‰ and −6.9‰. The deepest depth group (245–255 cm) showed the widest range between −10.6‰ and −6.2‰. Except for apparent outliers toward the end of the period illustrated (3 November to 1 December), most values fell within the calculated upper and lower confidence limits. Soil water $\delta^{2}H$ for the period illustrated ranged between −66.2‰ and 62.8‰ (Figure 4b).

### 3.2. Source Water Apportionment by Trees

Results from isotope mass balance calculations showed the following: initial soil water mass (91%) and total rainfall input mass (9%). Losses are partitioned into seepage (1%), interception (5%), soil water (91%), soil water evaporation (1%), and transpiration (2%). The sensitivity of our interception estimate (equation (7) in Text S1) resulting from $\delta_E$ (equation (8) in Text S1) was explored using the bootstrapped estimates shown in Table 1 and as specified in related text. The fraction of interception to the total water balance ranges between 0.0461 and 0.0479. We note possible sources of uncertainty in our water balance term estimates: (1) seepage—not all collector pipes produced water at the same time, and thus, it is not certain how much of the soil volume actually drained to those specific pipes, and (2) soil water storage—our depth-integrated estimates only spanned down to 150 cm, which is about half the entire soil depth.

The $\delta^{2}H$-$\delta^{18}O$ plot of seepage water, bulk soil water, and xylem water are shown in Figure 5, representing a cumulative observation duration of 70 days (30 September to 9 December 2014), that is, postdrought or during rewetting. The addition of a deuterated water (~152‰) to rainfall revealed three key patterns in δ-space, particularly during the first seven days of rewetting (30 September to 7 October): (1) most xylem water values stayed close to "background" −60‰ $\delta^{2}H$ during the first 24 hr (Figure 5a), about which time mixing between resident and incoming water in the bulk soil was apparent (−20‰ $\delta^{2}H$); (2) most xylem water values began moving up in the $\delta^{2}H$ axis (between ~−50‰ and ~−20‰; Figures 5b and 5c), effectively moving outside background concentrations, about which time mixing between resident and incoming water in the bulk soil continued (~10‰); and (3) contrast in tracer values, that is, labeled rainfall versus background values, showed a clear trend in that xylem water isotopic composition tracked the bulk soil water isotopic composition. When seepage water values began falling back to background (Figures 5d–5h), the contrast between the possible plant water sources dissipated. This period coincided with the time when VWC and SWP recovered back to predrought levels (Figure 3b).

Superimposing the isotope biplot in δ-space (Figure 5) with the Bayesian modeling results in proportion (i.e., p-space; Figure 6), an observation can be made that trees predominantly used soil water (89% ±6) and not the more mobile seepage water (11% ±6), particularly during the first 14 days of rewetting. As VWC and SWP recovered back to predrought levels between 7 and 14 October, bulk soil water use remained relatively high between 80% ±11 on 21 October and 72% ±10 on 9 December. Between resident (represented by pre-rewetting) soil water and newly mixed soil water (represented by three depth intervals), trees used 30% ±5 resident water and 19% ±5, 28% ±9, and 12% ±6 newly mixed water at respective depths during the first 14 days of rewetting. The fraction of more mobile seepage water remained relatively small (16% ±8)

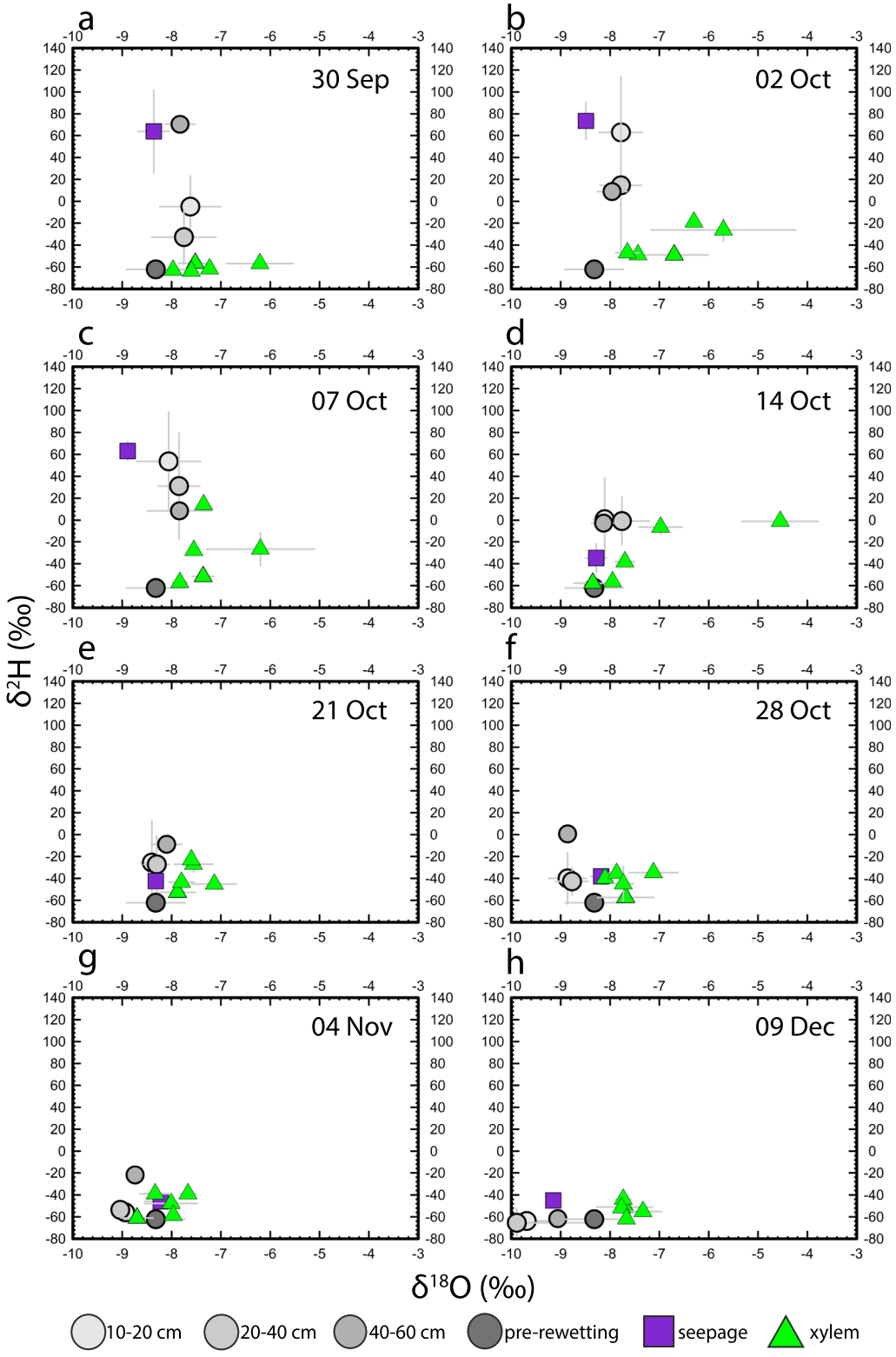


**Figure 5.** The $\delta^2$H-$\delta^{18}$O (δ-space) plot of xylem and possible source water end-members. (a–h) Results are presented per sampling time (30 September to 9 December). The first three end-members (10–20, 20–40, and 40–60 cm) are bulk soil values at respective sampling times, the fourth end-member (prerewetting) represents "resident" water using mean bulk soil values two weeks prior to rewetting, and the fifth end-member (seepage) represents "mobile" water. Symbols represent mean; error bars represent 1 SD.

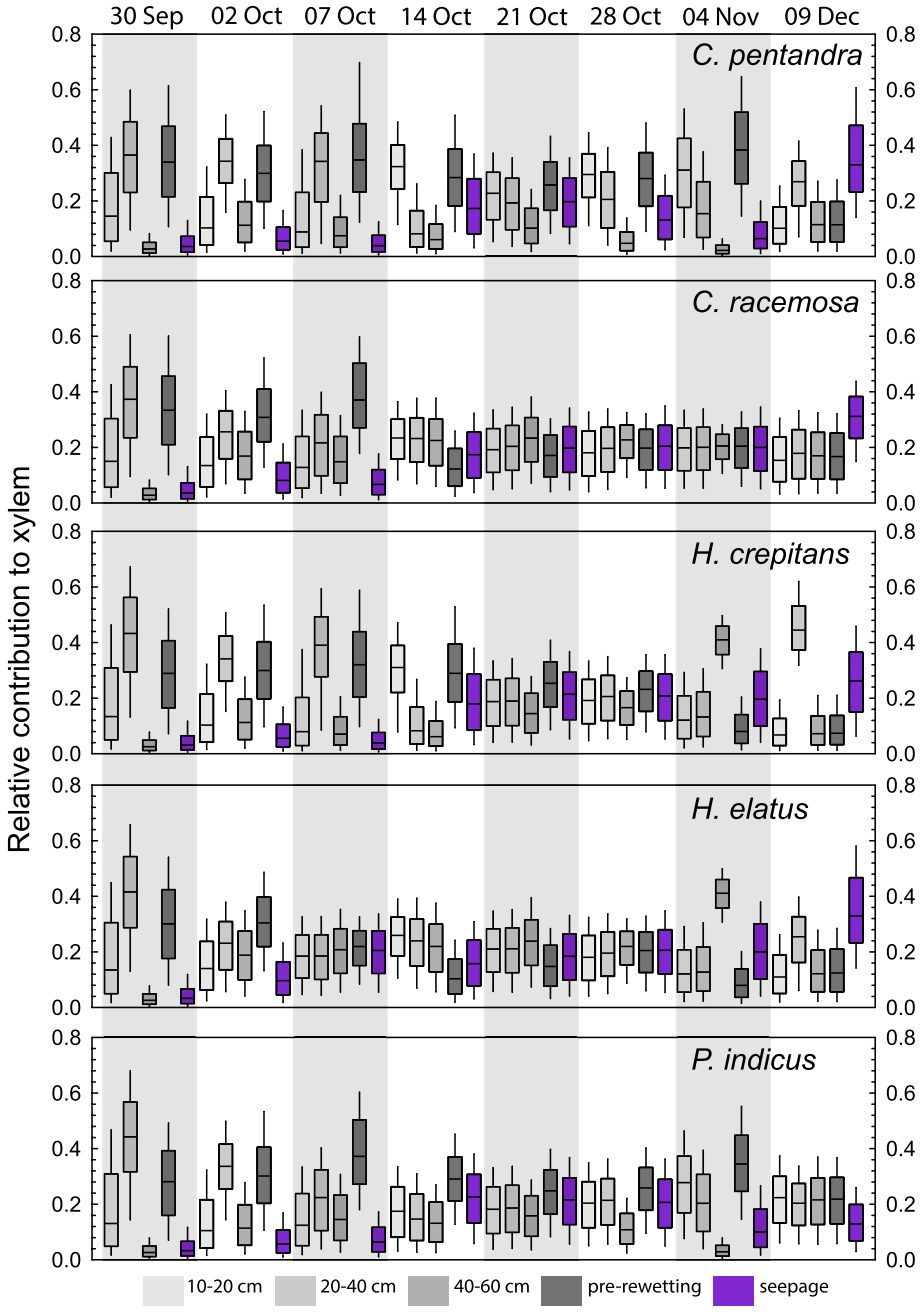


**Figure 6.** Source water partitioning using Bayesian mixing model (p-space). Results are grouped per species and sampling time. The first three end-members (10–20, 20–40, and 40–60 cm) are bulk soil values at respective sampling times, the fourth end-member (prerewetting) represents "resident" water using mean bulk soil values 2 weeks prior to rewetting, and the fifth end-member (seepage) represents "mobile" water.

through to the end of the period illustrated. Relatively minimal species-level differences in the percentage of seepage (more mobile) water are shown in Table 4, ranging between 14% ±7 (*P. indicus*) and 19% ±8 (*H. elatus*) over the period illustrated.

While results from source water apportionment and water balance models imply minimal use of more mobile seepage water, in relative proportions, seepage water in xylem was sampled disproportionally higher (16% ±8) than what was available in the seepage component of the water budget (i.e., 1% in seepage vs. 90% in soil water).

**Table 4**
*Xylem Water Source Proportions (Mean ± 1 SD) per Species for the Entire Period Illustrated in Figures 5 and 6*

| Species | 10–20 cm | 20–40 | 40–60 | Prerewetting | Seepage |
|---|---|---|---|---|---|
| *C. pentandra* | 0.22 ± 0.08 | 0.25 ± 0.09 | 0.09 ± 0.04 | 0.3 ± 0.08 | 0.15 ± 0.1 |
| *C. racemosa* | 0.18 ± 0.03 | 0.23 ± 0.06 | 0.18 ± 0.06 | 0.24 ± 0.09 | 0.17 ± 0.08 |
| *H. crepitans* | 0.17 ± 0.06 | 0.28 ± 0.13 | 0.14 ± 0.11 | 0.24 ± 0.1 | 0.16 ± 0.08 |
| *H. elatus* | 0.18 ± 0.04 | 0.23 ± 0.08 | 0.21 ± 0.1 | 0.19 ± 0.08 | 0.19 ± 0.08 |
| *P. indicus* | 0.2 ± 0.04 | 0.25 ± 0.09 | 0.13 ± 0.06 | 0.29 ± 0.05 | 0.14 ± 0.07 |

### 3.3. Transit Time and Flow Velocity

Time-variable forward and backward TTDs were estimated by transforming the maximum likelihood TTDs in the flow-weighted time space to calendar time space (Kim et al., 2016). While the forward and backward TTDs are more physically meaningful, the TTDs in the flow-weighted time were analyzed in this study because of the limited time variabilities on the estimated forward and backward TTDs imposed by the time-invariant flow pathway assumption, as well as the assumptions on the temporal structure of the outflux. Also, with the $\gamma$ parameter set as the mean flux rate, there is no scale difference between the flow-weighted TTDs and the TTDs in calendar time. More rigorous discussion on the time variability and its effect on the estimates are reserved for future study.

Overall, the analysis framework with the gamma distribution as a TTD in the flow-weighted time space was capable of resimulating the observed BTCs. The root-mean-square errors of the maximum likelihood simulations were 0.11, 0.02, 0.01, and 0.01 for the seepage, *C. racemosa*, *H. elatus*, and *H. crepitans*, respectively. The larger root-mean-square error of the resimulated seepage BTC was due to the incapability of simulating large fluctuations during the tracer injection periods which might be caused by time-varying flow pathways; however, the model was, at least, able to resimulate the general trend and the tailing of the observed BTC. The advection-dispersion model was also capable of resimulating observed concentration at the 0.25-m depth; the root-mean-square error of the modeled maximum likelihood concentration time series was 0.03.

The time scale differences among the waters that traveled through the different flow pathways (and indeed ended up in different outflux) were significant. In terms of MTT (Figure 7), the mean for the seepage flow

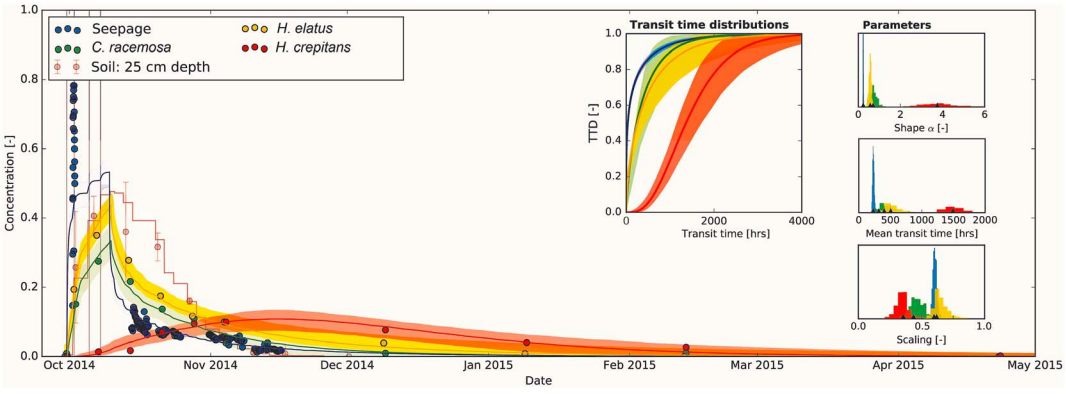


**Figure 7.** Observed and modeled breakthrough curves (BTCs) and estimated transit time distributions. Shaded gray vertical areas show the rainfall events with a $D_2O$ label. Observed BTCs are indicated with circles with different colors for each component. Modeled results are also shown with the same color scheme. (The line are the modeled BTCs with the maximum likelihood estimate parameter sets, and the shaded areas indicate the 95% highest posterior density [HPD] intervals.) The residence concentration time series at the 0.25-m depth is also shown with the 95% confidence interval of the measurements ($n = 3$) and the 95% HPD intervals of the resimulated concentration time series. The middle insert illustrates the cumulative transit time distributions with the associated 95% HPD intervals. Three subplots on the right are the posterior distributions of the model parameters with the triangles which indicate the maximum likelihood estimates. TTD = transit time distribution.

was the lowest and was around 215 hr [205, 250 hr] (~9 days). (All estimates in the Bayesian TTD modeling are reported with maximum likelihood estimates and 95% highest posterior density interval.) The MTTs for *C. racemosa* and *H. elatus* were quite similar to each other, 400 hr [245, 760 hr] (~17 days) and 505 hr [310, 880 hr] (~21 days), respectively. The estimated MTT at the 0.25 m below the soil surface was 330 hr [330, 340 hr] (~14 days), which is comparable to that of *C. racemosa* and *H. elatus. H. crepitans* transpired much older water, with a transpiration flux MTT of around 1,490 hr [1,160, 1,900 hr] (~62 days). Values of the shape parameter $\alpha$ of the TTDs for seepage, *H. elatus*, *C. racemosa*, and *H. crepitans* were 0.25 [0.23, 0.27], 0.70 [0.45, 1.27], 0.57 [0.44, 0.71], and 3.7 [2.3, 5.8], respectively. The estimated dispersivity at the soil depth was 0.015 m [0.013, 0.020 m]. We note that we excluded *C. pentandra* in TTD modeling because we did not detect any uptake of the tracer in the tree; that is, xylem $\delta^2$H remained relatively unchanged before, during, and after the drought at $-56$ ($\pm$4.5)‰. *P. indicus* was excluded in TTD modeling because, like *C. pentandra*, we did not detect any tracer uptake in the tree, as corroborated by apparent persistent use of "stream water" at all stages of the experiment (*P. indicus* is planted right by the meander of the "stream"; Figure 2a, top left corner).

The mass-recovery ratio for seepage and transpiration fluxes can be approximated based on the TTD modeling result in the absence of detailed information on outflux and relatively low sampling frequency of concentrations. According to the model, the mass-recovery ratio (the scaling factor) was about 60% [56%, 64%] for the seepage flux (i.e., about 60% of the tracer masses which took the flow pathway to the seepage was recovered), and 45% for transpiration flux on average (63% [56%, 78%] for *H. elatus*, 45% [36%, 58%] for *C. racemosa* ($n = 4$; the analyzed tree was assumed to be the representative of others), and 35% [24%, 44%] for *H. crepitans*). About 52% [48%, 56%] of tracer was recovered at the 0.25-m depth soil.

## 4. Discussion

Much of the presented analysis relied on the stable isotopes of water and the assumption that they are useful tools in tracing and partitioning various components of the water cycle, as others have done (e.g., Coenders-Gerrits et al., 2014; Ehleringer & Dawson, 1992; Evaristo & McDonnell, 2017; Gibson & Edwards, 2002; Jameel et al., 2016; Jasechko et al., 2013). Because of their conservative nature, we assume that stable isotopes of water are affected by physical processes that are relatively well understood (Dansgaard, 1964; Friedman, 1953). The general assumption that root water uptake, in most environments, is a nonfractionating process has been shown to be valid in both laboratory (Thorburn et al., 1993; Wershaw et al., 1966) and field (White et al., 1985) settings. Exceptions to this rule, however, have been reported in certain environments (Ellsworth & Williams, 2007; Evaristo et al., 2017; Lin & da Sternberg, 1993). Notwithstanding the long history in the use of water stable isotopes in root water uptake studies, dating back to the seminal work of Dawson and Ehleringer (1991), its *descriptive power* in hydrological models is still embryonic.

To assess ecohydrological separation, our study conducts and integrates novel approaches, including the following:

1. the use of a $D_2O$ label, following its evolution (i.e., breakthrough) in seepage (groundwater recharge), soils (soil water recharge), and trees (root water uptake);
2. sampling stem water for stable isotopes at high frequency; and
3. the application of TTD modeling in stem water isotopes over an extended period of over 6 months.

### 4.1. Ecohydrological Determinism in the Critical Zone?

By applying a root water uptake source apportionment model implemented in a Bayesian framework and by estimating "water ages" based on TTD modeling, we were able to provide the first evidence of ecohydrological separation in space and in time, respectively. We suggest that our rainfall labeling approach represents the plant water uptake system better than tree-based injection methods (Gaines et al., 2016; James et al., 2003) because it can "follow the water" from input as rainfall through to water uptake via roots. Equally noteworthy was our use of Bayesian inference methods in quantifying the sources of water used by trees after a prolonged drought. The main advantage of the Bayesian inference approach used here is that unlike previous work that has had to rely on the "offset" of a water sample from the local meteoric water line (e.g., Evaristo et al., 2015), or in earlier mixing model capabilities providing only "point estimates" (e.g., Brunel

et al., 1995), here we have a labeled source whose uncertainties as it is partitioned into various reservoirs prior to root water uptake are fully accounted for. The main advantage of the TTD modeling used here over tree-based injection work is that we have a full catchment description of transit times not only in trees but also in soils and seepage (proxy for groundwater recharge).

As with any isotope mixing model, the utility of a source water partitioning technique relies on the magnitude of difference between sources. At B2-TRF, isotopic differences are limited due to the relatively constant isotopic composition of the source groundwater well. Thus, the value of a labeled tracer—in both δ-space (Figure 5) and p-space (Figure 6)—cannot be overstated. We draw particular attention to the 30 September, 2 October, and 7 October sampling dates in both Figures 5 and 6, whereby the labeled tracer found its way out of the soil column as seepage (more mobile) water but only gradually and slowly into the bulk soil and xylem water. We interpret this as evidentiary support for ecohydrological separation, whereby trees used water in soil micropores instead of the more mobile, freely draining soil water that contributed to seepage. We argue that this finding would have remained obscured in the relatively small isotopic differences between the bulk soil and seepage water. Indeed, results from our source water apportionment model were more informative when applied after the rewetting (especially between 30 September and 14 October), highlighting both the utility of a labeled tracer and the limited applicability of a mixing model when end-member isotopic differences are small. Nonetheless, one overarching question remains: *why did trees not use mobile water when soils became wetter?*

Evaristo et al. (2015) proposed a conceptual mixing model (following Hrachowitz et al., 2013) informed only by the degree of separation between more mobile and less mobile waters—the line-conditioned excess (LCE) of Landwehr and Coplen (2006). The LCE parameter is not applicable in the B2-TRF because of (1) a rainfall isotopic composition that stays relatively constant all year round, (2) very limited evaporative demand (0.4 mm/day), and (3) labeled tracer addition. The first two factors lead to small natural variation of isotopic composition thereby making the dual-isotope approach, upon which the LCE parameter is derived, not applicable (Brunel et al., 1995). The B2-TRF system, therefore, is an ideal setup for a mechanistic assessment of ecohydrological separation. This is because root water uptake sources can be identified mainly on the basis of xylem water's isotopic "proximity" to its possible sources, without the potential complications in interpretation due to isotopic enrichment effects of soil water evaporation.

Under rewetting conditions, the dimensionless mixing coefficient $\boldsymbol{C_{M,i}}$ (equation (28) in Hrachowitz et al., 2013) that is controlled only by changes in soil moisture may explain our results in conceptual terms. That is, as the soil wets up, a decrease in soil matric potential leads to increasingly smaller proportions of tracer infiltrating the soil matrix, and thus increasingly greater proportions of the $D_2O$ label (new water) being routed to preferential flow pathways. The high flow velocities in preferential flow pathways result in earlier breakthroughs in seepage and therefore shorter MTTs (~10 days) than soil matrix water that is taken up by roots (17–62 days). Indeed, our soil matric potential measurements fully recovered to predrought levels (20–30 cm $H_2O$) ~14 days after the first postdrought rainfall. Overall, this supports an interpretation of a heightened ecohydrological separation in space (preference for soil matrix over preferential flow water) and in time (shorter transit times of preferential flow water than the water taken by roots).

Under drought conditions, we hypothesize a converse mechanism, whereby during dry-down due to root water uptake (Text S1 and Figure S1), the resultant and increasingly negative matric potential gradients in the rhizosphere would have directed the mobile water from pockets of larger pore spaces into refilling the site(s) of root water uptake in the soil matrix (Carminati et al., 2010; Daly et al., 2017). Following the Hrachowitz et al. (2013) model, such a drying condition would result in a higher dynamic mixing coefficient between the "refilling" mobile water that contributes to root water uptake and resident matrix water. These findings support the idea that antecedent soil moisture conditions and species-level response *determine* the partitioning between a more mobile and a less mobile water source for both vegetation and groundwater recharge.

Across changing soil moisture conditions, our results support an interpretation that ecohydrological separation was most marked at the transition from drought to rewetting, and negligible under drought conditions. While the latter interpretation is consistent with the Hrachowitz et al. (2013) model and the thought experiment of Berry et al. (2018), given the limited isotopic differences at B2-TRF outside the $D_2O$ labeling regime,

validating this interpretation presents an opportunity for future research. That is, ecohydrological separation may vary over time and environmental conditions (e.g., soil moisture) and with different site characteristics (e.g., more seepage).

Furthermore, we draw attention to possible implications of the relatively high proportion of seepage water in xylem (16% ±8) than what was available in the seepage component of the water budget (i.e., 1% seepage vs. 90% soil water). If we assume a setup whereby seepage water comprised a larger proportion of the water budget than the case was at B2-TRF, would that result in correspondingly larger proportion of seepage water in xylem, hence, a somewhat muted ecohydrological separation? The latter question opens an opportunity for future research.

### 4.2. On the Physical Meaning of "Tightly Bound Water"

The first paper on ecohydrological separation by Brooks et al. (2010) first introduced the phrase "tightly bound water" to describe the soil matrix water that is used by trees. Our study enabled us to clarify some of the implications of the so-called tightly bound water by providing evidence based on our soil and leaf water potential data, and Bayesian model of root water uptake sources. Following Smith and Sperry (2014), it can be shown that sap flow Q is related to transport driving force ΔP by hydraulic conductance K; that is, $Q = K \cdot \Delta P$. At a given Q, K is reduced as ΔP increases. Although we lack Q measurements, the decrease in leaf water potential for a given soil matric potential (increased ΔP) during drought could, in theory, lead to reduced K and greater risks for embolism (Smith & Sperry, 2014; Wheeler et al., 2013). This is not a surprise but rather simply demonstrates that *C. racemosa* was more "water stressed" than *H. elatus* (see section 4.3). These results suggest (and this is what we emphasize in this section) that there is no tightly bound water *sensu stricto* from a root water uptake perspective. Going forward, we enjoin the community to subscribe to Brantley et al.'s (2017) suggestion that matrix water—instead of "immobile," "bound," or tightly bound water—would be a more appropriate description of the water that does not flow freely under gravity. We suggest that such a conceptual and terminological qualification is necessary because, as demonstrated in this experiment, the water retained in the soil after a prolonged drought was not necessarily immobile insofar as root water uptake is concerned. Trees employ different strategies to changing soil moisture states that may have to do more with species-level controls than the "boundedness" of soil water. While cryogenic vacuum distillation method for soil water extraction represents suction pressures as high as $3 \times 10^{-8}$ MPa (Orlowski et al., 2016), this should not be interpreted as the region of suction pressures that drive water ascent in trees because trees can access water from water-filled pores that are too small for the roots (Brantley et al., 2017). Tightly bound water in the sense of Brooks et al. (2010), therefore, was a misnomer that we hope has been clarified by these results. Nonetheless, the use of the phrase tightly bound water was useful in differentiating cryogenically extracted water from the more mobile water as sampled from suction lysimeters.

### 4.3. Ecohydrological Separation in Space and in Time

The work presented here is the first evidence of ecohydrological separation that addresses the question whether or not the two water worlds is a separation in space or in time. As Bowen (2015) asked, "... the relative roles of physical and temporal segregation remain unclear. Do plants draw water from different parts of the soil matrix from groundwater recharge, or do plant withdrawals happen at a different time from groundwater recharge?"

Results from our Bayesian model of root water uptake suggest "space-based segregation." Model results show that the use of preferential flow (more mobile seepage) water remained relatively subdued throughout the rewetting period, ranging only between 5% and 28% of xylem water. If we qualify ecohydrological separation as vegetation using low mobility, soil matrix water over high mobility, preferential flow water (*sensu* Brooks et al., 2010), then our results confirm ecohydrological separation. This is (conceptually) consistent with the dynamic partial mixing mechanism of Hrachowitz et al. (2013); in that, the dynamic active storage below the root zone dominates preferential flow, while the dynamic passive storage around the root zone dominates soil matrix water. Notwithstanding, some nuances are apparent. Sixty percent of water in xylem was composed of resident (prerewetting) water and newly mixed water from 20–40 cm in approximately equal proportions. This suggests that "old" and "new" water were equally likely constituents of xylem water for these trees after a prolonged drought.

Results from our TTD modeling suggest a "time-based segregation"; that is, the water taken up by roots took a longer time to "exit" the tree than seepage water did in leaving the soil column by a factor of 2 to 7. The value of shape parameter $\alpha$ for seepage (0.23 [0.21, 0.25]) is at the lower end of the 0.3–0.7 range reported in many catchments in nature (Aubert et al., 2014; Godsey et al., 2010; Kirchner & Neal, 2013), representing rapid tracer release in seepage flux and subsequent lower tracer concentrations ~8 weeks after the first labeled rainfall. Parameter $\alpha$ was larger in *H. elatus* (0.70 [0.45, 1.27]) and *C. racemosa* (0.57 [0.44, 0.71]). The larger $\alpha$ in *H. elatus* and *C. racemosa* implies lesser variability in transit times of these outfluxes than in seepage. Consequently, skewness ($\mathbf{2}/\sqrt{\boldsymbol{\alpha}}$) and kurtosis ($\mathbf{6}/\boldsymbol{\alpha}$) were smaller in both species than in seepage. While we know of no study to date that used TTD modeling for xylem, the shape factors for *H. elatus* and *C. racemosa* fell well within the range of typical rainfall-runoff catchment TTDs (Kirchner, 2016). Notwithstanding, the differences in MTT is not trivial—seepage flux being almost a third of the average MTT for both species. Even more surprising is the TTD of *H. crepitans*, which rises to a peak after a long 6-week delay. We note, however, that while the broad family of gamma distributions for TT has been used widely elsewhere with success (Godsey et al., 2010; Jasechko et al., 2016; Kirchner, 2016; Kirchner et al., 2000), our adoption of the gamma distribution here is our first attempt at estimating transit times associated with transpiration. Future TT modeling work will consider time variability, caused by time-varying flow pathways (Harman, 2015; Harman & Kim, 2014; Kim et al., 2016).

Meanwhile, the estimated MTT at 0.25-m depth was longer (or at least similar regarding the uncertainty) than that of seepage flow, which occurred at 3-m depth. This could be attributed to the less mobile zone water sampled in the bulk soil. In other words, a large portion of the seepage flow was composed of water parcels that bypassed the soil collected in bulk samples, presumably traveling through the more mobile soil zone. This is also consistent with the estimated shape factor ($0.23\ [0.21, 0.25] \ll 1$) of the gamma TTD of the seepage flow, which implies much more dominant contribution of younger water to the seepage flow.

If we qualify ecohydrological separation strictly as a time-based segregation (*sensu* Bowen, 2015), then these MTT differences between seepage and transpiration fluxes may be interpreted as sampling of water from the same subsurface storage volume that differed only in average sampling flux, that is, transpiration water flux being slower than seepage flux by a factor of 2 to 7. An alternative interpretation, as discussed earlier, might be sampling of water from different subsurface compartments—transpiration from passive storage around the root zone (soil matrix water), seepage from active storage below the root zone (preferential flow water)—and different average sampling flux. The latter alternative explanation is more consistent with our definition of ecohydrological separation in this study, underpinned by the modeling approaches employed herein.

## 5. Conclusions

We presented an assessment of ecohydrological separation through a controlled drought and rainfall experiment at the Biosphere 2-Tropical Rainforest biome—a scale representative of a real-world critical zone setting, but with known and controlled boundary conditions. Specifically, we set out to answer the question, *is ecohydrological separation a separation in time or in space?* Our Bayesian mixing model of root water uptake sources showed that, particularly during rewetting, transpiration was derived from the less mobile soil matrix water, different to the more mobile water component in soils. This finding supports the conclusion that the source of transpiration water is preferential in space; hence, ecohydrological separation is a separation in space. Our TTD modeling of xylem and deep percolation water all showed that the water taken by roots was older than seepage ("groundwater recharge") water by a factor of 2 to 7. This finding supports the conclusion that ecohydrological separation is a separation in time. One possible explanation for these age differences is sourcing of transpiration and seepage water from the same storage volume but at markedly different average sampling flux. The Bayesian root water uptake and TTD modeling results presented here, however, are consistent with a perceptual (qualitative) model whereby transpiration is sourced from soil matrix (determined by antecedent moisture states and species-specific control) at a markedly different average sampling flux. The latter perceptual model may be implemented with future transit time modeling approaches that could account for unsteady fluxes and time-varying flow pathways. Finally, the space and time separation suggests that time-sensitive sampling techniques and modeling are of great importance to better understand the role of ecosystem components on the overall water cycle. The species-specific differences presented here suggest that we cannot treat trees as simple transport vessels, or straws.

**Acknowledgments**

Data used in the study can be obtained from HydroShare, https://doi.org/10.4211/hs.60fb3a408cac40cbb38b8f559ef1fc5c. All cryogenically extracted water samples (soil and xylem) are archived in McDonnell Lab; contact J. Evaristo (evaristo@sas.upenn.edu) for information on access to archived samples. We thank the following undergraduate research assistants for their help during the predrought and drought stages of the experiment: Meghan McDonnell, Ietza Gonzalez Silva, Fatima Olmos Flores, and Daniel Espinosa Ruiz. We thank Maggie Heard, Sara Jane Harders, John Adams, Kim Land, and all staff and crew at Biosphere 2 for their invaluable support during the conduct of this experiment. Peter Troch acknowledges funding from the Agnese N. Haury Foundation. Finally, we thank Kim Janzen and Cody Millar in McDonnell Lab (University of Saskatchewan, SK, Canada) for the logistical and lab support and Gibson Lab (University of Victoria, BC, Canada) for the mass spectrometry analysis. J. Evaristo thanks Saskatchewan Innovation and Opportunity Scholarship (Government of Saskatchewan) and Graduate Research Fellowship (School of Environment and Sustainability) for the research funding. The overall funding for this project is from an NSERC Discovery Grant and Accelerator Award to J. J. M.

## References

Ali, M., Fiori, A., & Russo, D. (2014). A comparison of travel-time based catchment transport models, with application to numerical experiments. *Journal of Hydrology*, *511*, 605–618. https://doi.org/10.1016/j.jhydrol.2014.02.010

Arain, M., Shuttleworth, W., Farnsworth, B., Adams, J., & Sen, O. (2000). Comparing micrometeorology of rain forests in Biosphere-2 and Amazon basin. *Agricultural and Forest Meteorology*, *100*(4), 273–289. https://doi.org/10.1016/S0168-1923(99)00153-7

Aubert, A. H., Kirchner, J. W., Gascuel-Odoux, C., Faucheux, M., Gruau, G., & Merot, P. (2014). Fractal water quality fluctuations spanning the periodic table in an intensively farmed watershed. *Environmental Science & Technology*, *48*(2), 930–937. https://doi.org/10.1021/es403723r

Berry, Z. C., Evaristo, J., Moore, G., Poca, M., Steppe, K., Verrot, L., et al. (2018). The two water worlds hypothesis: Addressing multiple working hypotheses and proposing a way forward. *Ecohydrology*, *11*(3), e1843. https://doi.org/10.1002/eco.1843

Bowen, G. (2015). HYDROLOGY the diversified economics of soil water. *Nature*, *525*(7567), 43–44. https://doi.org/10.1038/525043a

Bowling, D. R., Schulze, E. S., & Hall, S. J. (2016). Revisiting streamside trees that do not use stream water: Can the two water worlds hypothesis and snowpack isotopic effects explain a missing water source? *Ecohydrology*. https://doi.org/10.1002/eco.1771

Brantley, S. L., Eissenstat, D. M., Marshall, J. A., Godsey, S. E., Balogh-Brunstad, Z., Karwan, D. L., et al. (2017). Reviews and syntheses: On the roles trees play in building and plumbing the critical zone. *Biogeosciences*, *14*(22), 5115–5142. https://doi.org/10.5194/bg-14-5115-2017

Brooks, J. R. (2015). Water, bound and mobile. *Science*, *349*(6244), 138–139. https://doi.org/10.1126/science.aac4742

Brooks, J. R., Barnard, H. R., Coulombe, R., & McDonnell, J. J. (2010). Ecohydrologic separation of water between trees and streams in a Mediterranean climate. *Nature Geoscience*, *3*(2), 100–104. https://doi.org/10.1038/ngeo722

Brunel, J. P., Walker, G. R., & Kennettsmith, A. K. (1995). Field validation of isotopic procedures for determining sources of water used by plants in a semiarid environment. *Journal of Hydrology*, *167*(1-4), 351–368. https://doi.org/10.1016/0022-1694(94)02575-V

Carminati, A., Moradi, A. B., Vetterlein, D., Vontobel, P., Lehmann, E., Weller, U., et al. (2010). Dynamics of soil water content in the rhizosphere. *Plant and Soil*, *332*(1-2), 163–176. https://doi.org/10.1007/s11104-010-0283-8

Coenders-Gerrits, A. M. J., van der Ent, R. J., Bogaard, T. A., Wang-Erlandsson, L., Hrachowitz, M., & Savenije, H. H. G. (2014). Uncertainties in transpiration estimates. *Nature*, *506*(7487), E1–E2. https://doi.org/10.1038/nature12925

Craig, H., & Gordon, L. I. (1965). Deuterium and oxygen 18 variations in the ocean and marine atmosphere. In E. Tongiorgi (Ed.), *Stable isotopes in oceanographic studies and paleotemperatures* (pp. 9–130). Pisa, Italy: Lab. Geologia Nucleare.

Daly, K. R., Cooper, L. J., Koebernick, N., Evaristo, J., Keyes, S. D., van Veelen, A., & Roose, T. (2017). Modelling water dynamics in the rhizosphere. *Rhizosphere*, *4*, 139–151. https://doi.org/10.1016/j.rhisph.2017.10.004

Dansgaard, W. (1964). Stable isotopes in precipitation. *Tellus*, *16*, 436–468.

Dawson, T. E. (1993). Hydraulic lift and water use by plants: Implications for water balance, performance and plant-plant interactions. *Oecologia*, *95*(4), 565–574. https://doi.org/10.1007/BF00317442

Dawson, T. E., & Ehleringer, J. R. (1991). Streamside trees that do not use stream water. *Nature*, *350*(6316), 335–337. https://doi.org/10.1038/350335a0

Ehleringer, J. R., & Dawson, T. E. (1992). Water uptake by plants: Perspectives from stable isotope composition. *Plant, Cell and Environment*, *15*(9), 1073–1082. https://doi.org/10.1111/j.1365-3040.1992.tb01657.x

Ellsworth, P. Z., & Williams, D. G. (2007). Hydrogen isotope fractionation during water uptake by woody xerophytes. *Plant and Soil*, *291*(1-2), 93–107. https://doi.org/10.1007/s11104-006-9177-1

Evaristo, J., Jasechko, S., & McDonnell, J. J. (2015). Global separation of plant transpiration from groundwater and streamflow. *Nature*, *525*(7567), 91–94. https://doi.org/10.1038/nature14983

Evaristo, J., & McDonnell, J. J. (2017). Prevalence and magnitude of groundwater use by vegetation: A global stable isotope meta-analysis. *Scientific Reports*, *7*(1), 44110. https://doi.org/10.1038/srep44110

Evaristo, J., McDonnell, J. J., & Clemens, J. (2017). Plant source water apportionment using stable isotopes: A comparison of simple linear, two-compartment mixing model approaches. *Hydrological Processes*, *31*(21), 3750–3758. https://doi.org/10.1002/hyp.11233

Evaristo, J., McDonnell, J. J., Scholl, M. A., Bruijnzeel, L. A., & Chun, K. P. (2016). Insights into plant water uptake from xylem-water isotope measurements in two tropical catchments with contrasting moisture conditions. *Hydrological Processes*, *30*(18), 3210–3227. https://doi.org/10.1002/hyp.10841

Friedman, I. (1953). Deuterium content of natural waters and other substances. *Geochimica et Cosmochimica Acta*, *4*(1-2), 89–103. https://doi.org/10.1016/0016-7037(53)90066-0

Gaines, K. P., Meinzer, F. C., Duffy, C. J., Thomas, E. M., & Eissenstat, D. M. (2016). Rapid tree water transport and residence times in a Pennsylvania catchment. *Ecohydrology*, *9*(8), 1554–1565. https://doi.org/10.1002/eco.1747

Geris, J., Tetzlaff, D., McDonnell, J., Anderson, J., Paton, G., & Soulsby, C. (2015). Ecohydrological separation in wet, low energy northern environments? A preliminary assessment using different soil water extraction techniques. *Hydrological Processes*, *29*(25), 5139–5152. https://doi.org/10.1002/hyp.10603

Gibson, J. J., & Edwards, T. W. D. (2002). Regional water balance trends and evaporation-transpiration partitioning from a stable isotope survey of lakes in northern Canada. *Global Biogeochemical Cycles*, *16*(2), 1026. https://doi.org/10.1029/2001GB001839

Godsey, S. E., Aas, W., Clair, T. A., de Wit, H. A., Fernandez, I. J., Kahl, J. S., et al. (2010). Generality of fractal 1/*f* scaling in catchment tracer time series, and its implications for catchment travel time distributions. *Hydrological Processes*, *24*(12), 1660–1671. https://doi.org/10.1002/hyp.7677

Goldsmith, G. R., Muñoz-Villers, L. E., Holwerda, F., Mcdonnell, J. J., Asbjornsen, H., & Dawson, T. E. (2012). Stable isotopes reveal linkages among ecohydrological processes in a seasonally dry tropical montane cloud forest. *Ecohydrology*, *5*(6), 779–790. https://doi.org/10.1002/eco.268

Good, S. P., Noone, D., & Bowen, G. (2015). Hydrologic connectivity constrains partitioning of global terrestrial water fluxes. *Science*, *349*(6244), 175–177. https://doi.org/10.1126/science.aaa5931

Hall, S. J., Weintraub, S. R., & Bowling, D. R. (2016). Scale-dependent linkages between nitrate isotopes and denitrification in surface soils: Implications for isotope measurements and models. *Oecologia*, 1–11.

Harman, C. J. (2015). Time-variable transit time distributions and transport: Theory and application to storage-dependent transport of chloride in a watershed. *Water Resources Research*, *51*, 1–30. https://doi.org/10.1002/2014WR015707

Harman, C. J., & Kim, M. (2014). An efficient tracer test for time-variable transit time distributions in periodic hydrodynamic systems. *Geophysical Research Letters*, *41*, 1567–1575. https://doi.org/10.1002/2013GL058980

Hervé-Fernández, P., Oyarzún, C., Brumbt, C., Huygens, D., Bodé, S., Verhoest, N. E. C., & Boeckx, P. (2016). Assessing the "two water worlds" hypothesis and water sources for native and exotic evergreen species in south-central Chile. *Hydrological Processes*. https://doi.org/10.1002/hyp.10984

Hrachowitz, M., Benettin, P., van Breukelen, B. M., Fovet, O., Howden, N. J. K., Ruiz, L., et al. (2016). Transit times—The link between hydrology and water quality at the catchment scale. *Wiley Interdisciplinary Reviews Water*, *3*(5), 629–657. https://doi.org/10.1002/wat2.1155

Hrachowitz, M., Fovet, O., Ruiz, L., & Savenije, H. H. G. (2015). Transit time distributions, legacy contamination and variability in biogeochemical 1/*f* (alpha) scaling: How are hydrological response dynamics linked to water quality at the catchment scale? *Hydrological Processes*, *29*(25), 5241–5256. https://doi.org/10.1002/hyp.10546

Hrachowitz, M., Savenije, H., Bogaard, T. A., Tetzlaff, D., & Soulsby, C. (2013). What can flux tracking teach us about water age distribution patterns and their temporal dynamics? *Hydrology and Earth System Sciences*, *17*(2), 533–564. https://doi.org/10.5194/hess-17-533-2013

Jameel, Y., Brewer, S., Good, S. P., Tipple, B. J., Ehleringer, J. R., & Bowen, G. J. (2016). Tap water isotope ratios reflect urban water system structure and dynamics across a semiarid metropolitan area. *Water Resources Research*, *52*, 5891–5910. https://doi.org/10.1002/2016WR019104

James, S., Meinzer, F., Goldstein, G., Woodruff, D., Jones, T., Restom, T., et al. (2003). Axial and radial water transport and internal water storage in tropical forest canopy trees. *Oecologia*, *134*(1), 37–45. https://doi.org/10.1007/s00442-002-1080-8

Jasechko, S., Kirchner, J. W., Welker, J. M., & McDonnell, J. J. (2016). Substantial proportion of global streamflow less than three months old. *Nature Geoscience*, *9*(2), 126–129. https://doi.org/10.1038/ngeo2636

Jasechko, S., Sharp, Z. D., Gibson, J. J., Birks, S. J., Yi, Y., & Fawcett, P. J. (2013). Terrestrial water fluxes dominated by transpiration. *Nature*, *496*(7445), 347–350. https://doi.org/10.1038/nature11983

Kim, M., Pangle, L. A., Cardoso, C., Lora, M., Volkmann, T. H. M., Wang, Y., et al. (2016). Transit time distributions and StorAge selection functions in a sloping soil lysimeter with time-varying flow paths: Direct observation of internal and external transport variability. *Water Resources Research*, *52*, 7105–7129. https://doi.org/10.1002/2016WR018620

Kirchner, J., Feng, X., & Neal, C. (2000). Fractal stream chemistry and its implications for contaminant transport in catchments. *Nature*, *403*(6769), 524–527. https://doi.org/10.1038/35000537

Kirchner, J. W. (2016). Aggregation in environmental systems—Part 1: Seasonal tracer cycles quantify young water fractions, but not mean transit times, in spatially heterogeneous catchments. *Hydrology and Earth System Sciences*, *20*(1), 279–297. https://doi.org/10.5194/hess-20-279-2016

Kirchner, J. W., & Neal, C. (2013). Universal fractal scaling in stream chemistry and its implications for solute transport and water quality trend detection. *Proceedings of the National Academy of Sciences of the United States of America*, *110*(30), 12,213–12,218. https://doi.org/10.1073/pnas.1304328110

Klaus, J., Chun, K. P., McGuire, K. J., & McDonnell, J. J. (2015). Temporal dynamics of catchment transit times from stable isotope data. *Water Resources Research*, *51*, 4208–4223. https://doi.org/10.1002/2014WR016247

Landwehr, J. M., & Coplen, T. B. (2006). Line-conditioned excess: a new method for characterizing stable hydrogen and oxygen isotope ratios in hydrologic systems. In *International Conference on Isotopes in Environmental Studies, 5 Aquatic Forum, Monte-Carlo, Monaco, 25-29 October 2004* (pp. 132–135). Vienna: IAEA.

Leigh, L., Burgess, T., Marino, B., & Wei, Y. (1999). Tropical rainforest biome of Biosphere 2: Structure, composition and results of the first 2 years of operation. *Ecological Engineering*, *13*(1-4), 65–93. https://doi.org/10.1016/S0925-8574(98)00092-5

Lin, G., & da Sternberg, L. S. L. (1993). Hydrogen isotopic fractionation by plant roots during water uptake in coastal wetland plants. In J. R. Ehleringer, A. E. Hall, & G. D. Farquhar (Eds.), *Stable isotopes and plant carbon-water relations* (pp. 497–510). New York: Academic Press Inc. https://doi.org/10.1016/B978-0-08-091801-3.50041-6

Maxwell, R. M., & Condon, L. E. (2016). Connections between groundwater flow and transpiration partitioning. *Science*, *353*(6297), 377–380. https://doi.org/10.1126/science.aaf7891

McCutcheon, R. J., McNamara, J. P., Kohn, M. J., & Evans, S. L. (2017). An evaluation of the ecohydrological separation hypothesis in a semiarid catchment. *Hydrological Processes*, *31*(4), 783–799. https://doi.org/10.1002/hyp.11052

McDonnell, J. J. (2014). The two water worlds hypothesis: Ecohydrological separation of water between streams and trees? *WIREs Water*, *1*(4), 323–329. https://doi.org/10.1002/wat2.1027

McDonnell, J. J., & Beven, K. (2014). Debates—The future of hydrological sciences: A (common) path forward? A call to action aimed at understanding velocities, celerities and residence time distributions of the headwater hydrograph. *Water Resources Research*, *50*, 5342–5350. https://doi.org/10.1002/2013WR015141

McDonnell, J. J., Evaristo, J., Bladon, K. D., Buttle, J., Creed, I. F., Dymond, S. F., et al. (2018). Water sustainability and watershed storage. *Nature Sustainability*, *1*(8), 378–379. https://doi.org/10.1038/s41893-018-0099-8

McDonnell, J. J., McGuire, K., Aggarwal, P., Beven, K. J., Biondi, D., Destouni, G., et al. (2010). How old is streamwater? Open questions in catchment transit time conceptualization, modelling and analysis. *Hydrological Processes*, *24*(12), 1745–1754. https://doi.org/10.1002/hyp.7796

McGuire, K. J., & McDonnell, J. J. (2006). A review and evaluation of catchment transit time modeling. *Journal of Hydrology*, *330*(3-4), 543–563. https://doi.org/10.1016/j.jhydrol.2006.04.020

McGuire, K. J., & McDonnell, J. J. (2015). Tracer advances in catchment hydrology. *Hydrological Processes*, *29*(25), 5135–5138. https://doi.org/10.1002/hyp.10740

Meinzer, F., Brooks, J., Domec, J., Gartner, B., Warren, J., Woodruff, D., et al. (2006). Dynamics of water transport and storage in conifers studied with deuterium and heat tracing techniques. *Plant, Cell & Environment*, *29*(1), 105–114. https://doi.org/10.1111/j.1365-3040.2005.01404.x

Ogle, K., Tucker, C., & Cable, J. M. (2014). Beyond simple linear mixing models: Process-based isotope partitioning of ecological processes. *Ecological Applications*, *24*(1), 181–195. https://doi.org/10.1890/12-1970.1

Ogle, K., Wolpert, R., & Reynolds, J. (2004). Reconstructing plant root area and water uptake profiles. *Ecology*, *85*(7), 1967–1978. https://doi.org/10.1890/03-0346

Orlowski, N., Breuer, L., & McDonnell, J. J. (2016). Critical issues with cryogenic extraction of soil water for stable isotope analysis. *Ecohydrology*, *9*(1), 3–10. https://doi.org/10.1002/eco.1722

Parnell, A. C., Inger, R., Bearhop, S., & Jackson, A. L. (2010). Source partitioning using stable isotopes: Coping with too much variation. *PLoS ONE*, *5*(3), e9672. https://doi.org/10.1371/journal.pone.0009672

Phillips, D. L., & Gregg, J. W. (2003). Source partitioning using stable isotopes: Coping with too many sources. *Oecologia*, *136*(2), 261–269. https://doi.org/10.1007/s00442-003-1218-3

Phillips, D. L., Inger, R., Bearhop, S., Jackson, A. L., Moore, J. W., Parnell, A. C., et al. (2014). Best practices for use of stable isotope mixing models in food-web studies. *Canadian Journal of Zoology*, *92*(10), 823–835. https://doi.org/10.1139/cjz-2014-0127

Phillips, S. L., & Ehleringer, J. R. (1995). Limited uptake of summer precipitation by Bigtooth maple (Acer-Grandidentatum Nutt) and Gambels oak (Quercus-Gambelii Nutt). *Trees-Structure and Function*, *9*, 214–219.

Rascher, U., Bobich, E. G., Lin, G. H., Walter, A., Morris, T., Naumann, M., et al. (2004). Functional diversity of photosynthesis during drought in a model tropical rainforest - the contributions of leaf area, photosynthetic electron transport and stomatal conductance to reduction in net ecosystem carbon exchange. *Plant, Cell & Environment*, *27*(10), 1239–1256. https://doi.org/10.1111/j.1365-3040.2004.01231.x

Rosolem, R., Shuttleworth, W. J., Zeng, X., Saleska, S. R., & Huxman, T. E. (2010). Land surface modeling inside the Biosphere 2 tropical rain forest biome. *Journal of Geophysical Research*, *115*, G04035. https://doi.org/10.1029/2010JG001443

Schlesinger, W. H., & Jasechko, S. (2014). Transpiration in the global water cycle. *Agricultural and Forest Meteorology*, *189*, 115–117.

Scott, H. (1999). Characteristics of soils in the tropical rainforest biome of Biosphere 2 after 3 years. *Ecological Engineering*, *13*(1-4), 95–106. https://doi.org/10.1016/S0925-8574(98)00093-7

Smith, D. D., & Sperry, J. S. (2014). Coordination between water transport capacity, biomass growth, metabolic scaling and species stature in co-occurring shrub and tree species. *Plant, Cell & Environment*, *37*(12), 2679–2690. https://doi.org/10.1111/pce.12408

Soulsby, C., Birkel, C., & Tetzlaff, D. (2016). Characterizing the age distribution of catchment evaporative losses. *Hydrological Processes*, *30*(8), 1308–1312. https://doi.org/10.1002/hyp.10751

Sprenger, M., Leistert, H., Gimbel, K., & Weiler, M. (2016). Illuminating hydrological processes at the soil-vegetation-atmosphere interface with water stable isotopes. *Reviews of Geophysics*, *54*, 674–704. https://doi.org/10.1002/2015RG000515

Sutanto, S. J., Wenninger, J., Coenders-Gerrits, A. M. J., & Uhlenbrook, S. (2012). Partitioning of evaporation into transpiration, soil evaporation and interception: A comparison between isotope measurements and a HYDRUS-1D model. *Hydrology and Earth System Sciences*, *16*(8), 2605–2616. https://doi.org/10.5194/hess-16-2605-2012

Tetzlaff, D., Buttle, J., Carey, S. K., van Huijgevoort, M. H. J., Laudon, H., McNamara, J. P., et al. (2015). A preliminary assessment of water partitioning and ecohydrological coupling in northern headwaters using stable isotopes and conceptual runoff models. *Hydrological Processes*, *29*(25), 5153–5173. https://doi.org/10.1002/hyp.10515

Thorburn, P. J., & Walker, G. R. (1994). Variations in stream water uptake by *Eucalyptus camaldulensis* with differing access to stream water. *Oecologia*, *100*(3), 293–301. https://doi.org/10.1007/BF00316957

Thorburn, P. J., Walker, G. R., & Brunel, J. P. (1993). Extraction of water from Eucalyptus trees for analysis of deuterium and O-18—Laboratory and field techniques. *Plant, Cell & Environment*, *16*(3), 269–277. https://doi.org/10.1111/j.1365-3040.1993.tb00869.x

Wershaw, R. L., Friedman, I., & Heller, S. J. (1966). Hydrogen isotope fractionation of water passing through trees. In F. Hobson & M. Speers (Eds.), *Advances in organic geochemistry* (pp. 55–67). New York: Pergamon.

Wheeler, J. K., Huggett, B. A., Tofte, A. N., Rockwell, F. E., & Holbrook, N. M. (2013). Cutting xylem under tension or supersaturated with gas can generate PLC and the appearance of rapid recovery from embolism. *Plant, Cell & Environment*, *36*, 1938–1949.

White, J. W. C., Cook, E. R., Lawrenc, J. R., & Broecker, W. S. (1985). The deuterium to hydrogen ratios of sap in trees: Implications for water sources and tree ring deuterium to hydrogen ratios. *Geochimica et Cosmochimica Acta*, *49*(1), 237–246. https://doi.org/10.1016/0016-7037(85)90207-8

Wilusz, D. C., Harman, C. J., & Ball, W. P. (2017). Sensitivity of catchment transit times to rainfall variability under present and future climates. *Water Resources Research*, *53*, 10,231–10,256. https://doi.org/10.1002/2017WR020894

Zhang, Z. Q., Evaristo, J., Li, Z., Si, B. C., & McDonnell, J. J. (2017). Tritium analysis shows apple trees may be transpiring water several decades old. *Hydrological Processes*, *31*(5), 1196–1201. https://doi.org/10.1002/hyp.11108

## References from The Supporting Information

Brooks, R.H., & Corey, A. T. (1964). Hydraulic properties of porous media, Hydrology Papers, No.3, Colorado State University, Fort Collins, Colorado.

Cox, D. R., & Reid, N. (1987). Parameter orthogonality and approximate conditional inference. *Journal of the Royal Statistical Society: Series B: Methodological*, *49*(1), 1–18. https://doi.org/10.1111/j.2517-6161.1987.tb01422.x

Efron, B. (1981). Nonparametric standard errors and confidence intervals. *The Canadian Journal of Statistics*, *9*(2), 139–158. https://doi.org/10.2307/3314608

Ellsworth, T. R., Shaouse, P. J., Jobes, J. A., Fargerlund, J., & Skaggs, T. H. (1996). Solute transport in unsaturated soil: Experimental design, parameter estimation, and model discrimination. *Soil Science Society of America Journal*, *60*(2), 397–407. https://doi.org/10.2136/sssaj1996.03615995006000020010x

Harman, C. J., Ward, A. S., & Ball, A. (2016). How does reach-scale stream-hyporheic transport vary with discharge? Insights from rSAS analysis of sequential tracer injections in a headwater mountain stream. *Water Resources Research*, *52*, 7130–7150. https://doi.org/10.1002/2016WR018832

Hrachowitz, M., Soulsby, C., Tetzlaff, D., Malcolm, I. A., & Schoups, G. (2010). Gamma distribution models for transit time estimation in catchments: Physical interpretation of parameters and implications for time-variant transit time assessment. *Water Resources Research*, *46*, W10536. https://doi.org/10.1029/2010WR009148

Kirchner, J. W., Tetzlaff, D., & Soulsby, C. (2010). Comparing chloride and water isotopes as hydrological tracers in two Scottish catchments. *Hydrological Processes*, *24*(12), 1631–1645. https://doi.org/10.1002/hyp.7676

Kreft, A., & Zuber, A. (1978). On the physical meaning of the dispersion equation and its solutions for different initial and boundary conditions. *Chemical Engineering Science*, *33*(11), 1471–1480. https://doi.org/10.1016/0009-2509(78)85196-3

Parker, J. C., & vanGenuchten, M. T. (1984). Flux-averaged and volume-averaged concentrations in continuum approaches to solute transport. *Water Resources Research*, *20*(7), 866–872. https://doi.org/10.1029/WR020i007p00866

Rubin, D. B. (1981). The Bayesian bootstrap. *The Annals of Statistics*, *9*(1), 130–134.

Schoups, G., & Vrugt, J. A. (2010). A formal likelihood function for parameter and predictive inference of hydrologic models with correlated, heteroscedastic, and non-Gaussian errors. *Water Resources Research*, *46*, W10531. https://doi.org/10.1029/2009WR008933

Vrugt, J. A., ter Braak, C. J. F., Diks, C. G. H., Robinson, B. A., Hyman, J. M., & Higdon, D. (2009). Accelerating Markov chain Monte Carlo simulation by differential evolution with self-adaptive randomized subspace sampling. *International Journal of Nonlinear Sciences and Numerical Simulation*, *10*, 273–290.

## Erratum

In the originally published version of this article, Figure 7 was incorrect. The figure has since been corrected, and this version may be considered the authoritative version of record.